Computer Aided Multiscale Design of SiC-Si_3N_4 Nanoceramic Composites for High-Temperature Structural Applications

PIs: Vikas Tomar[1] and John E Renaud[2]

[1]School of Aeronautics and Astronautics
Purdue University, West Lafayette-Indiana, USA, 47907

[2]Aerospace and Mechanical Engineering
University of Notre Dame, Notre Dame-Indiana, USA, 46556

Program Manager: Dr. Patricia Rawls

DoE-NETL UCR Grant DE-FG26-07NT43072

Students

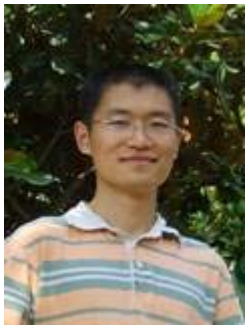

Gilberto Meja-Rodriguez, Devendra Dubey, Ming Gan, Vikas Samvedi

Collaborators

John Renaud (Material Design), Raj Bordia (Material Processing and Manufacturing)

Lab Facilities

52 Processor Opteron dual core supercomputing cluster, 8 Terabytes storage server, Veeco AFM, MTS Instron mechanical hydraulic testing machine, Hopkinson bar for dynamic high strain rate testing

Motivation

- **$SiC-Si_3N_4$ Nanocomposites**
  - **Evidence in literature that both fracture toughness and creep resistance can be improved in the case of $SiC-Si_3N_4$ nanocomposites Niihara, Mukherjee etc.**
  - **Multiscale microstructure**

- **Polymer-Derived Ceramics (PDCs)**
  - **A novel way to process si based ceramics**
  - **Micro-structure and properties can be further tailored by adding filler particles**

		cubic-SiC:	β-Si_3N_4:
Creep resistance (High Temp.)		✓	×
Strength	Room Temp.	✓	✓
	High Temp.	✓	✓
Toughness (High Temp.)		×	✓

Few Micrographs

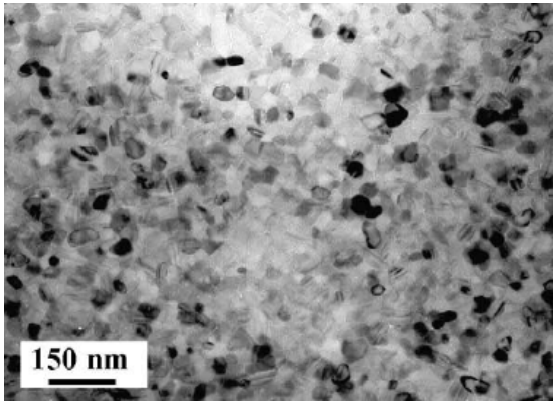

30 SC

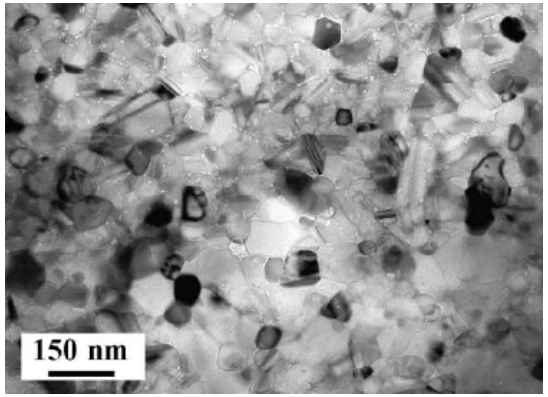

20 SC

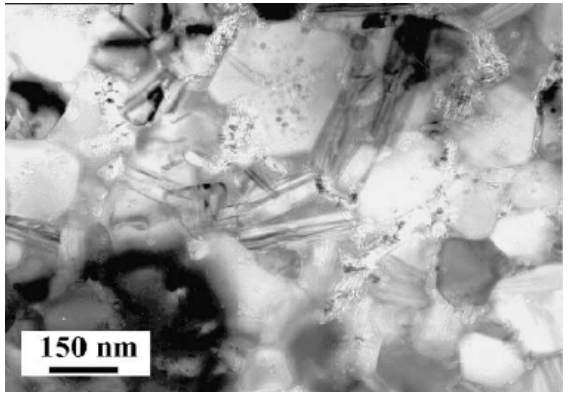

10 SC

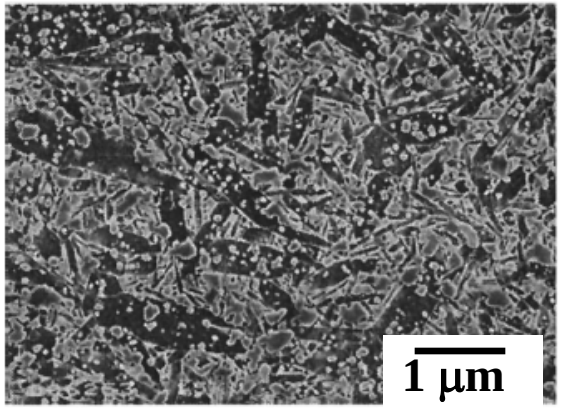

20SC

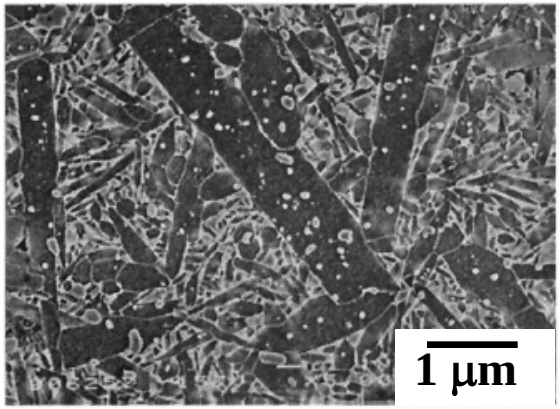

5SC

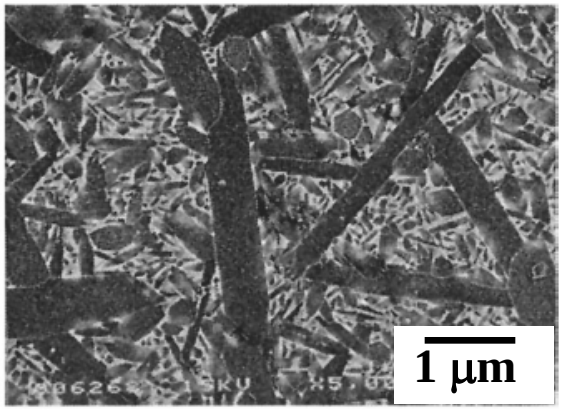

100SN

Interfaces

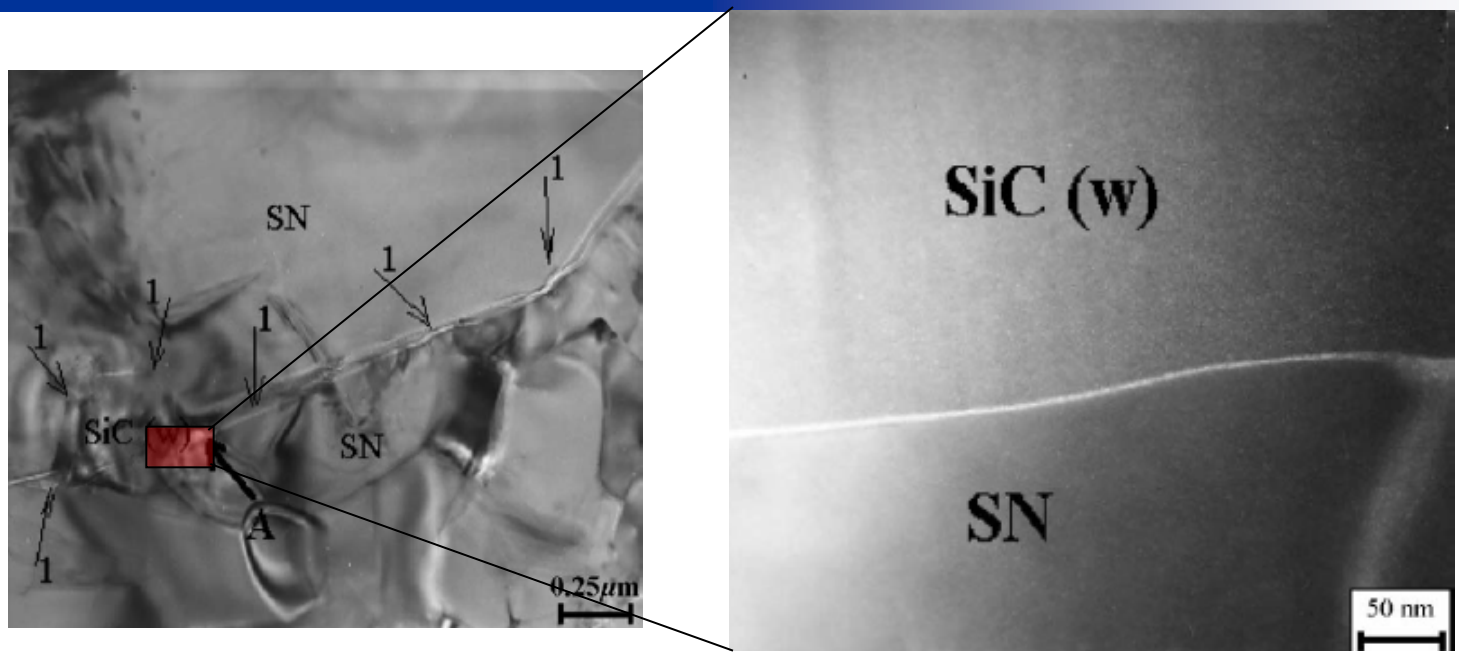

1

2

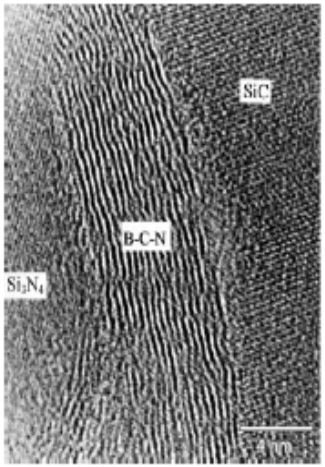

3

Set-UP

Experiments

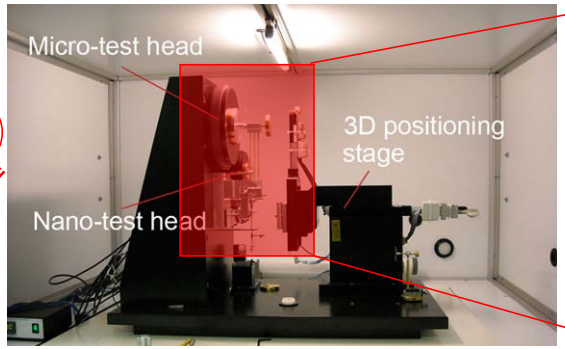

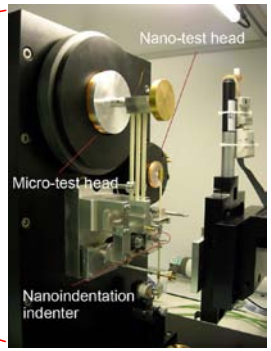

Experimental Microstructure

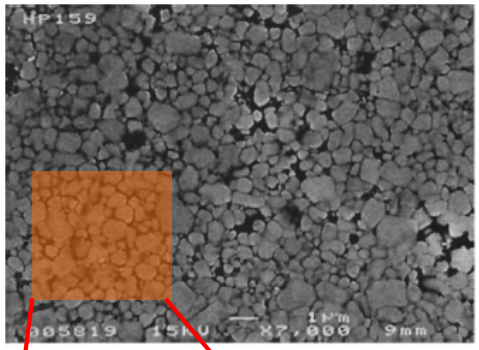

5

Finite Element

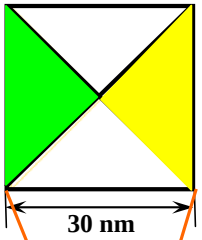

2

Molecular Models of Interfaces To Derive Finite Element Properties

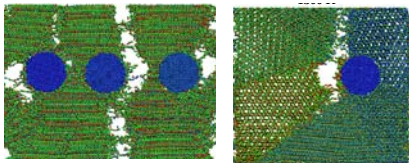

1

Grain Boundary

3

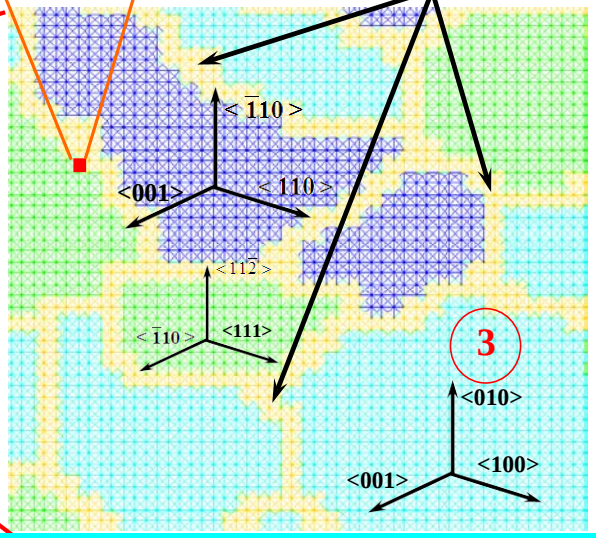

4

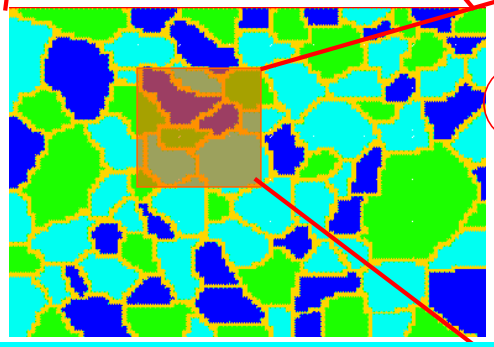

Finite Element Representation Based on Experimental Microstructural Characterization

Detailed View of Finite Element Mesh with Explicit GB and Orientation Representation

Outline

- **High temperature creep and nanoindentation experiments**
  - **Scale dependent nanoindentation upto 773 K**
  - **Nanoscale creep at different strain rates and maximum load**
- **Cohesive finite element based modeling of dynamic fracture failure in SiC-Si_3N_4 nanocomposites**
  - **Cohesive analyses accounting for second phase particle distribution and grain boundary distribution effects**
  - **High temperature constitutive models and trade-offs in designing these materials for high temperature performance**
- **Insights from molecular analyses**
  - **Nanoscale fracture and strength at room temperature**
  - **Role of temperature in strength upto 1500 K**
- **Designing materials in an optimization framework**

Experimental Investigations

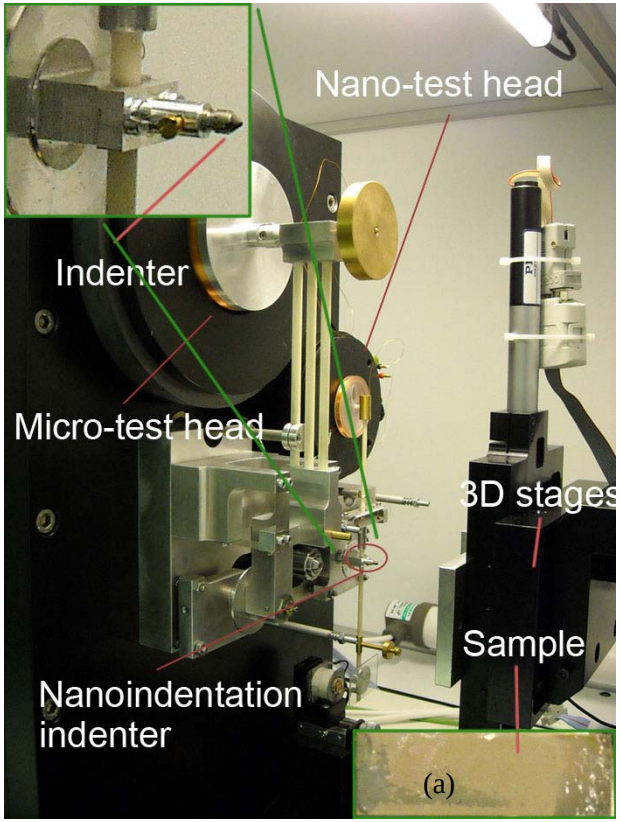

(a)

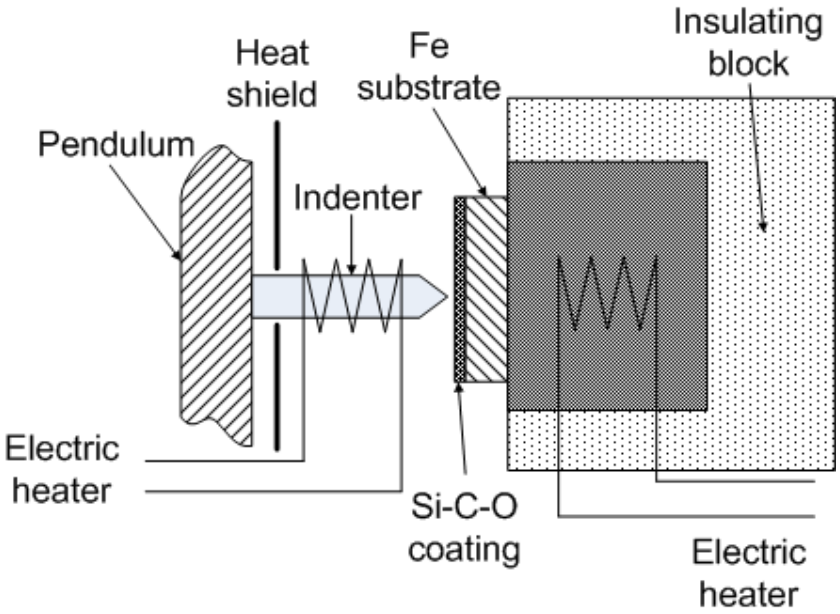

(b)

Deformation Visualization

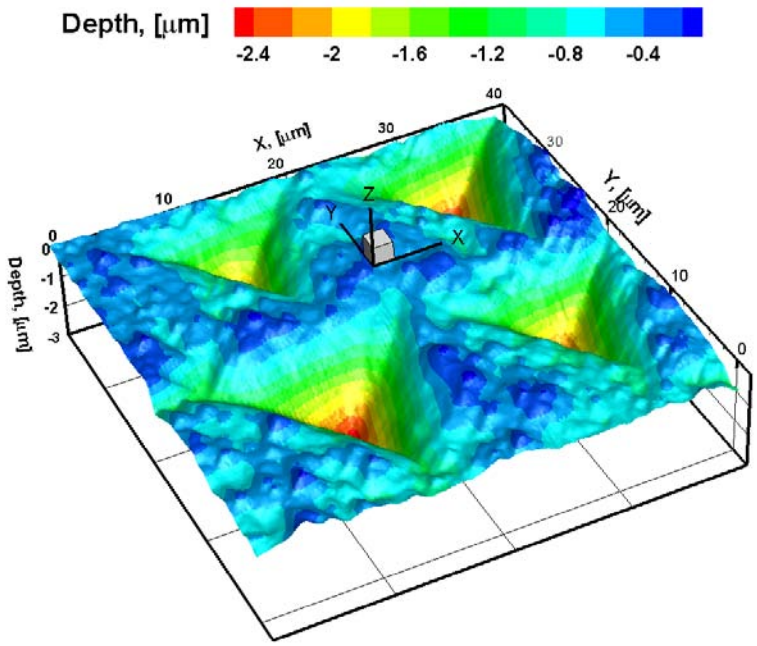

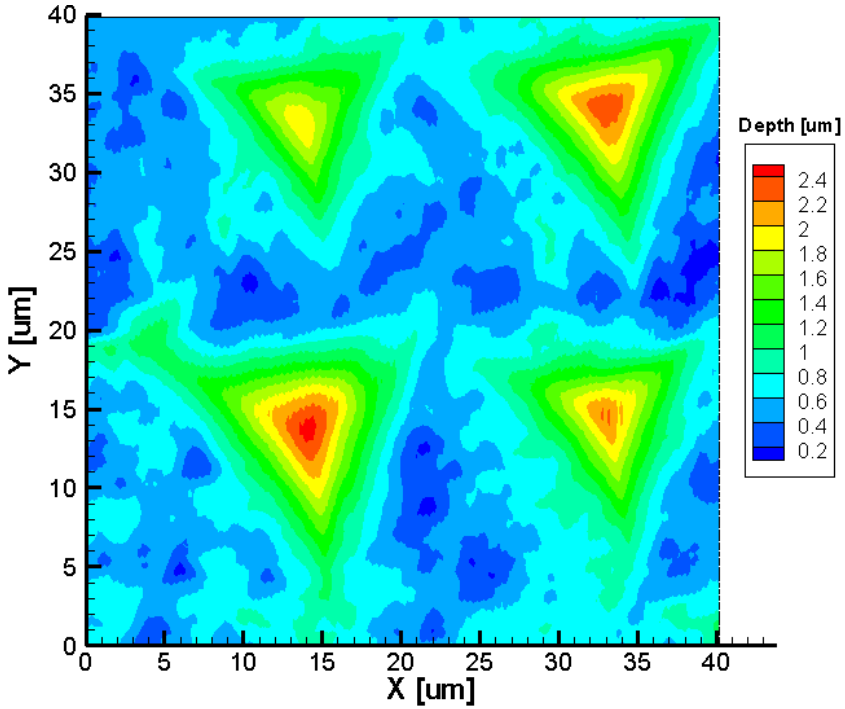

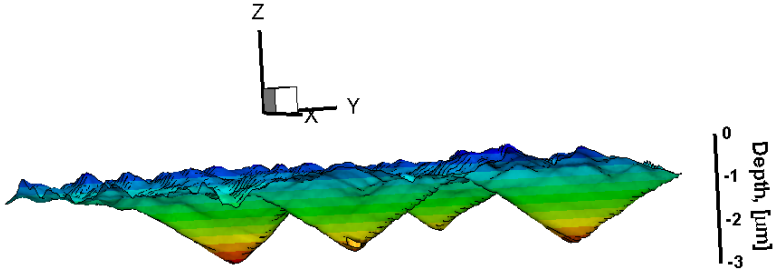

Multiscale Temperature Dependent Moduli

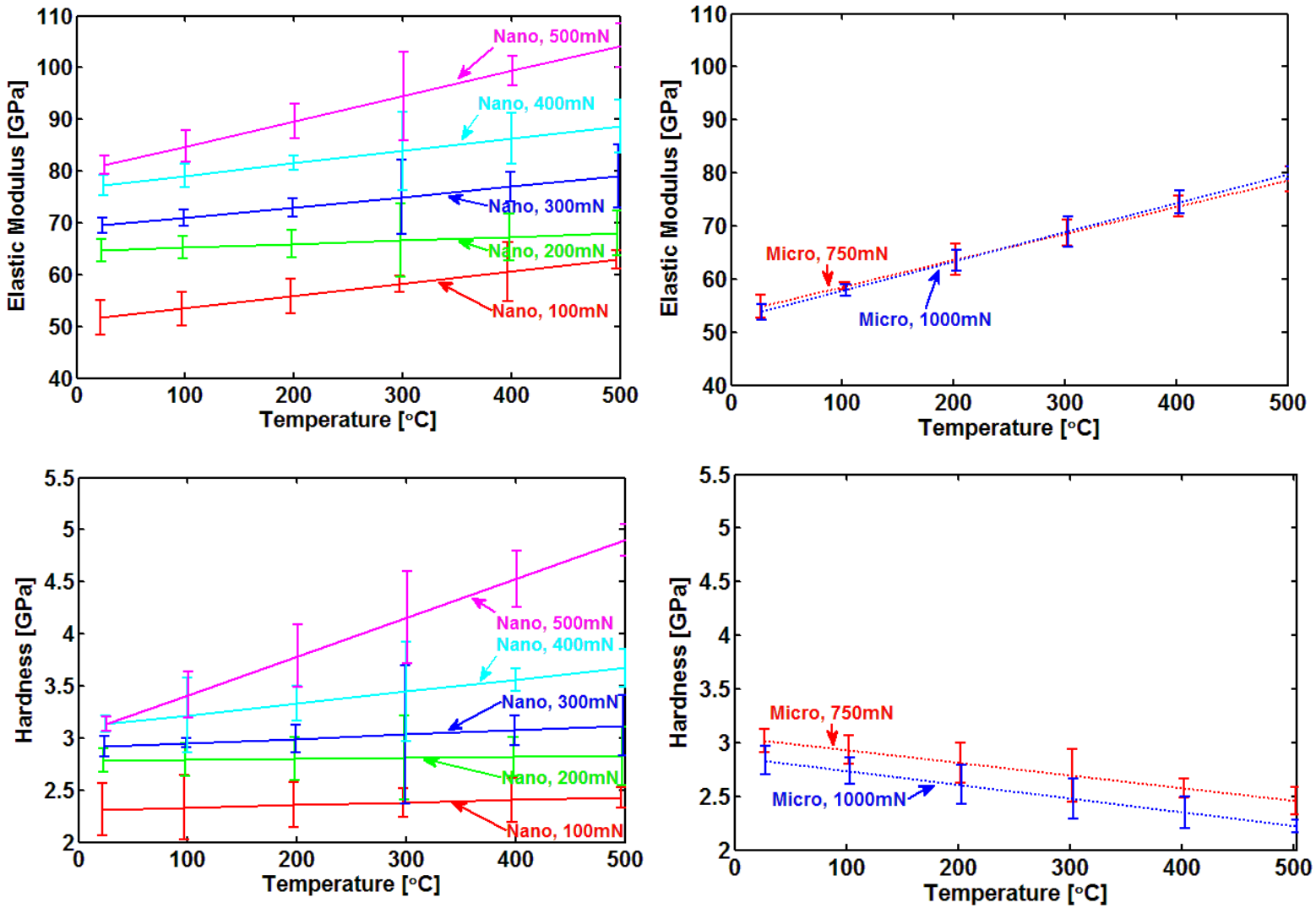

Issue of Thermal Drift

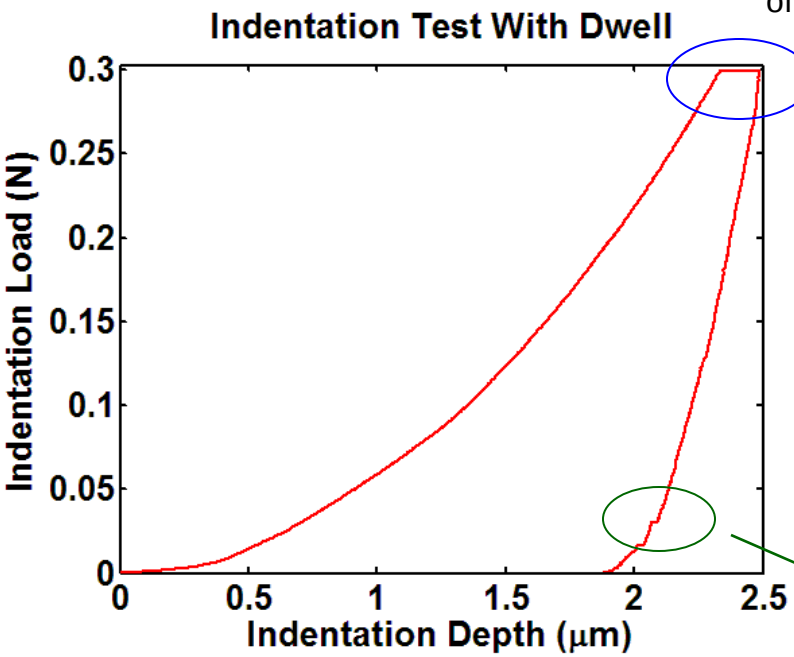

Monitoring depth change as a function of time

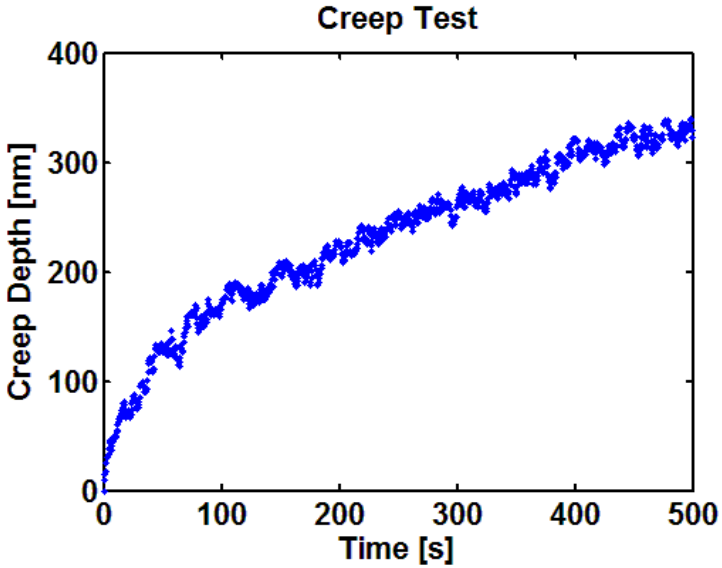

This thermal drift correction is applied to both indentation and creep

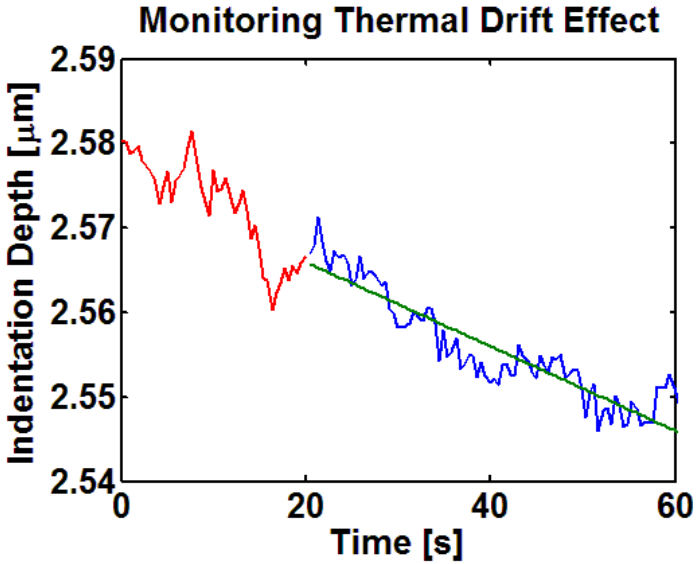

Thermal Drift at Nano and Micron Scales

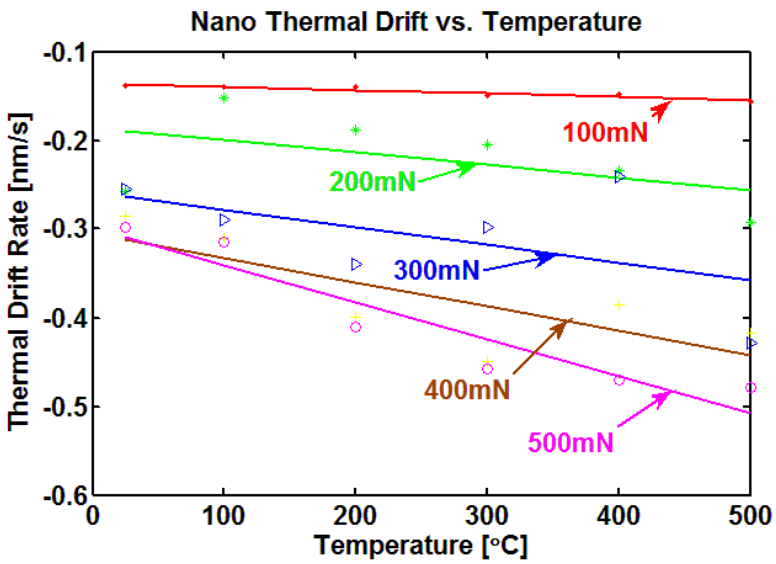

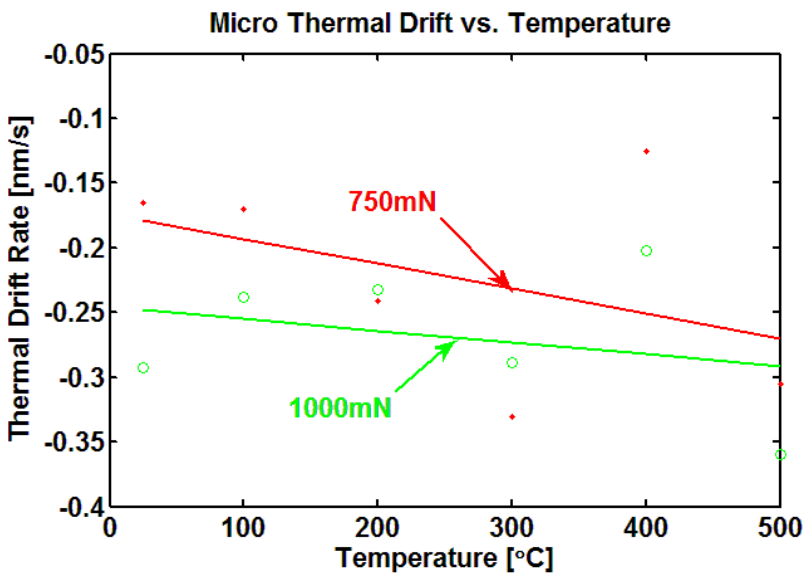

Thermal Drift rate changes as a function of both temperature and load

The drift values at different load/temperature are fitted linearly to show this relationship

Creep Models

From classical mechanisms of creep deformation, creep is a consequence of dislocation motion or diffusion.

$$\dot{\varepsilon}_s = \dot{\varepsilon}_0 \left(\frac{\sigma}{\sigma_0}\right)^n \left(\frac{D}{D_0}\right)^m \exp\left(-\frac{Q}{RT}\right)$$

Dislocation controlled creep: *n*= 3 to 5, *m*=0
Diffusional controlled creep: *n* ≈1,*m*= -3 to -2

$$\dot{\varepsilon}_c = A\sigma^n \exp\left(-\frac{Q}{RT}\right) \qquad \dot{\varepsilon}_s = \frac{\dot{\varepsilon}_0}{\eta_0} \frac{V_f^3}{\left(1-V_f\right)^2} \sigma \exp\left(\alpha\sigma\right) \exp\left(-\frac{Q}{RT}\right)$$

diffusion **Cavities**

Creep Measurements (h vs. t)

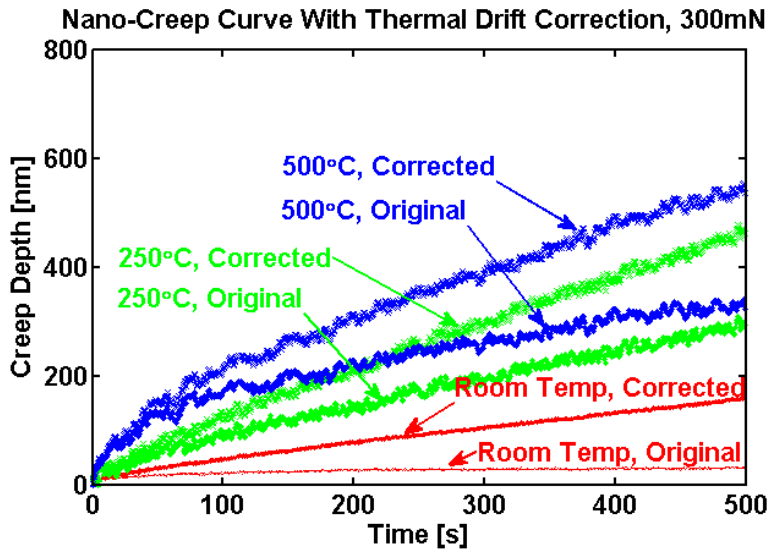

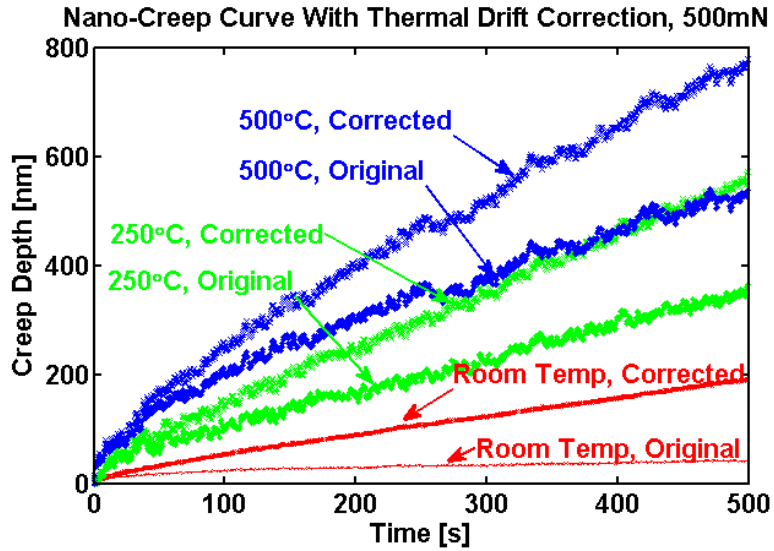

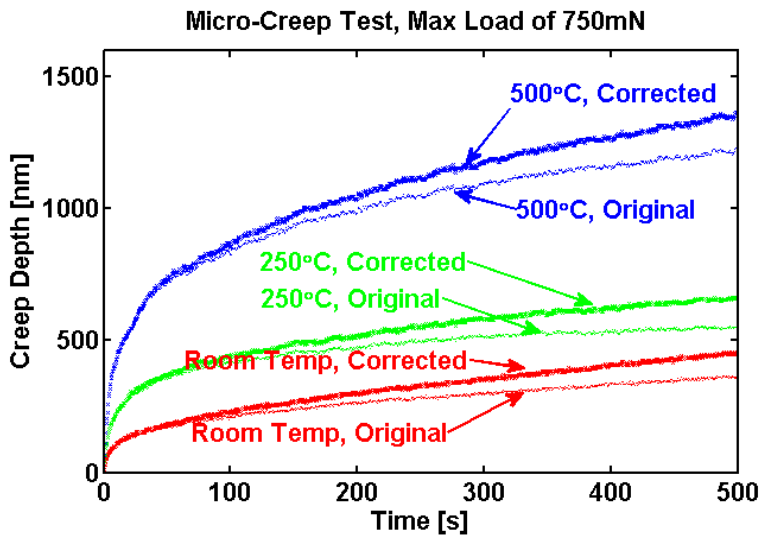

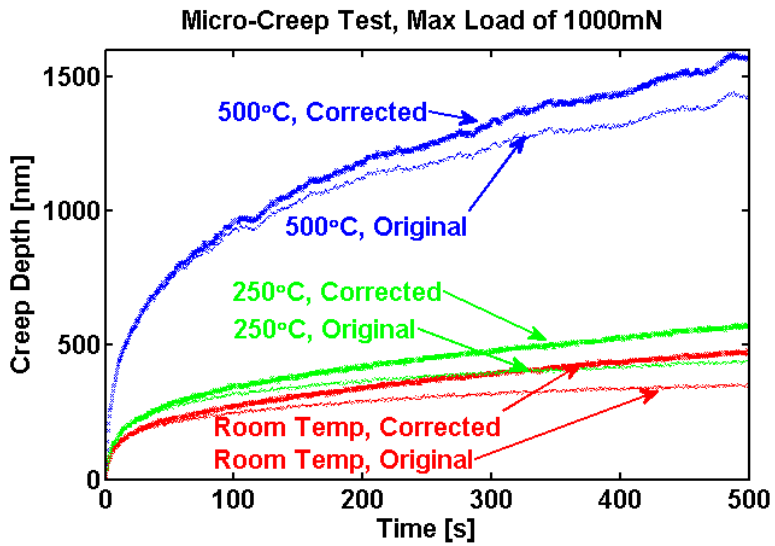

Exponent and Strain Rate

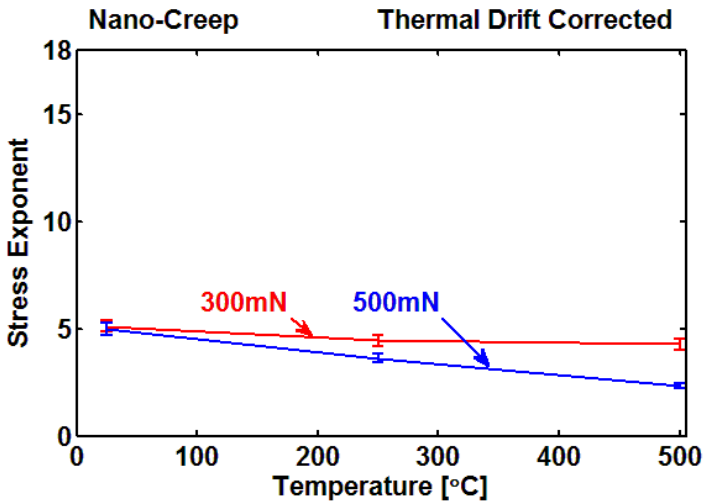

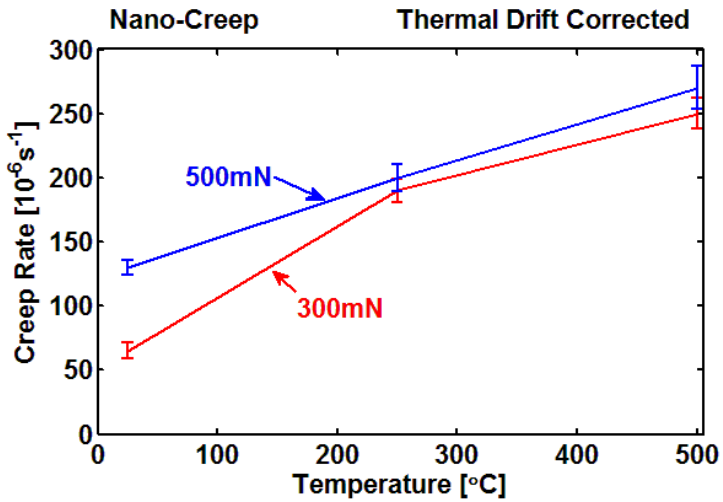

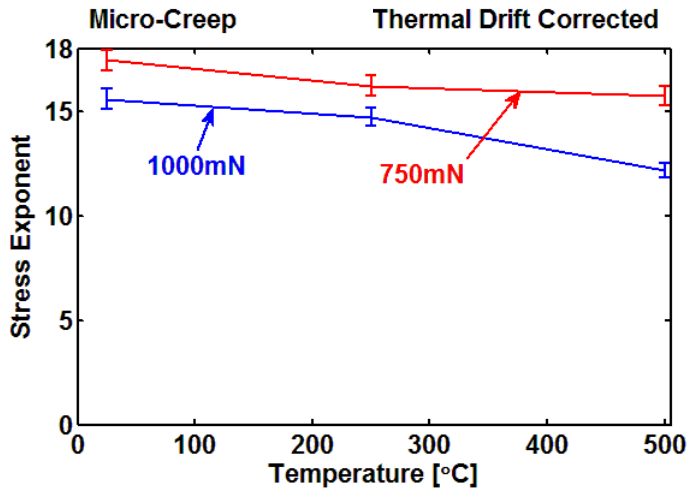

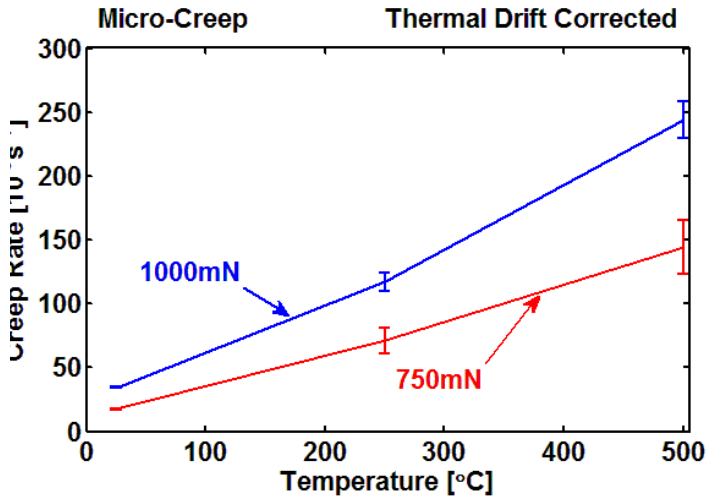

Outline

- High temperature creep and nanoindentation experiments in high temperature composites
  - Scale dependent nanoindentation upto 773 K
  - Nanoscale creep at different strain rates and maximum load
- **Cohesive finite element based modeling of dynamic fracture failure in SiC-Si_3N_4 nanocomposites**
  - **Cohesive analyses accounting for second phase particle distribution and grain boundary distribution effects**
  - **High temperature constitutive models and trade-offs in designing these materials for high temperature performance**
- Insights from molecular analyses
  - Nanoscale fracture and strength at room temperature
  - Role of temperature in strength upto 1500 K
- Designing materials in an optimization framework

Idealized Microstructural Representation

Real Microstructure

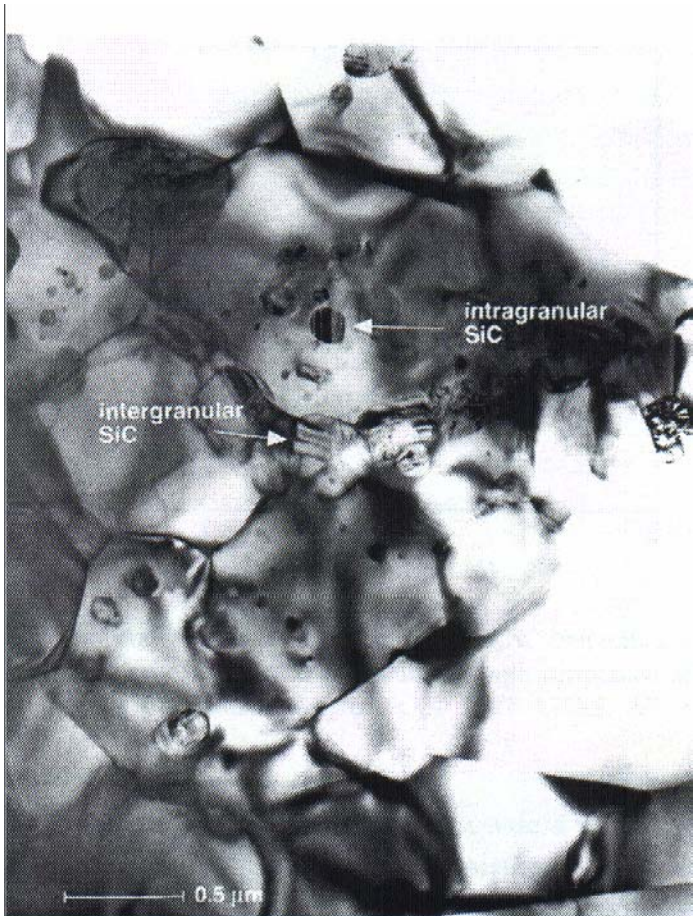

Hypothetical Microstructure

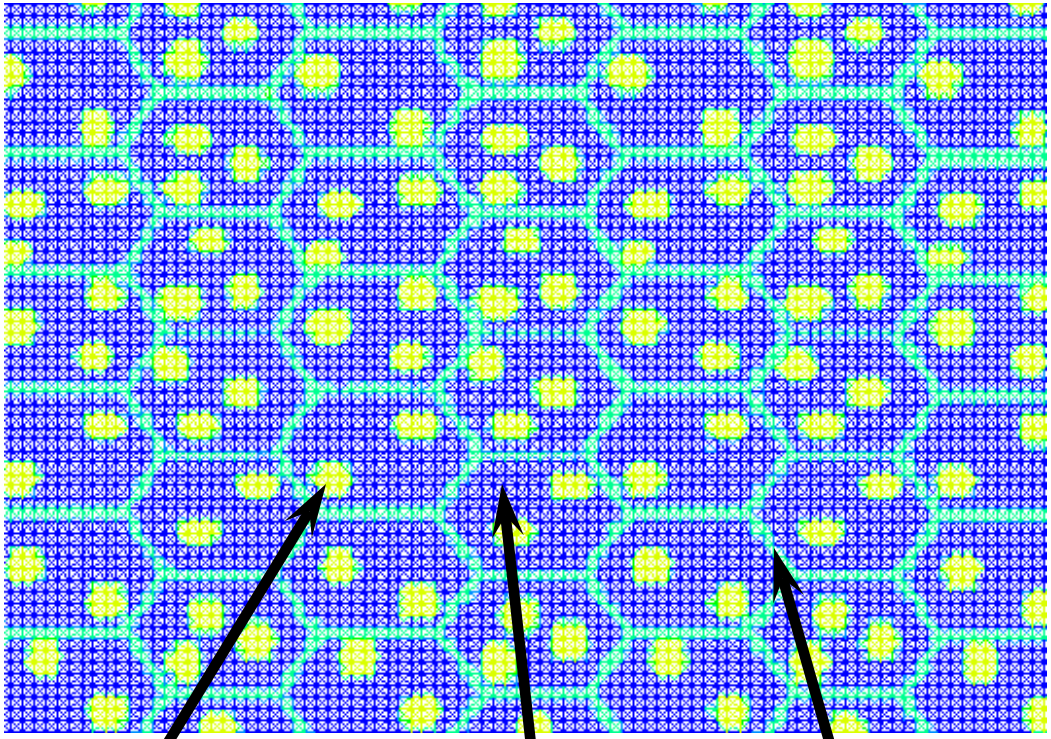

Silicon Carbide Silicon Nitride GB

AIAA, SDM-2007, Paper No. AIAA-2007-2345

Engg. Fract Mech. 2008, Mod. Sim. Mat. Sci. Engg. 2008

DE-FG26-07NT43072: Program Manager Dr. Patricia Rawls

Set-UP

Experiments

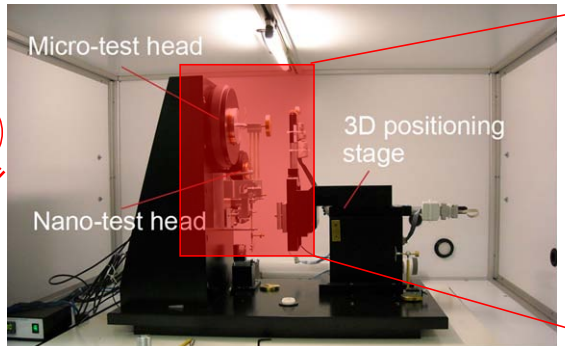

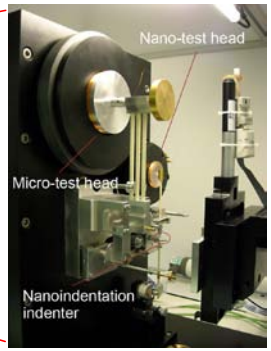

Experimental Microstructure

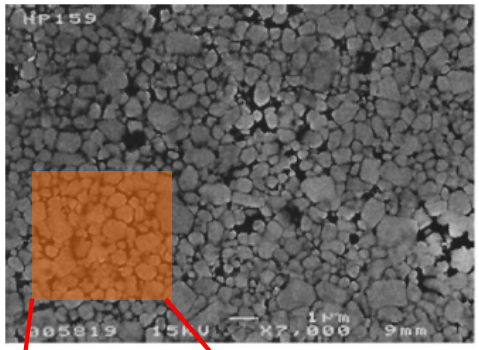

5

Finite Element

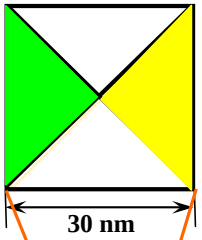

2

Molecular Models of Interfaces To Derive Finite Element Properties

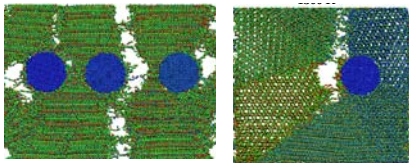

1

Grain Boundary

3

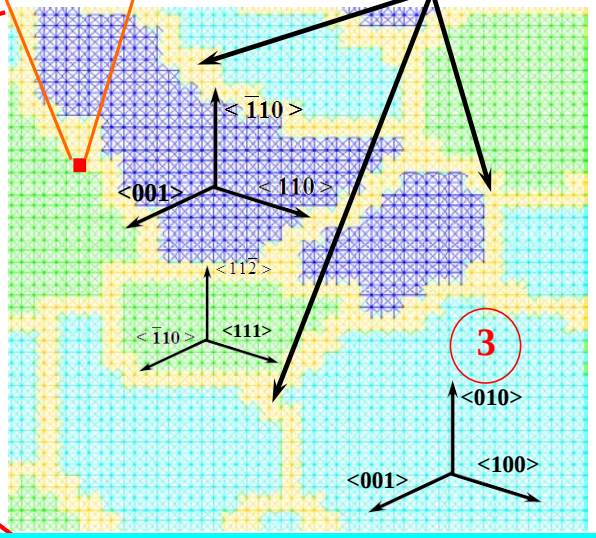

4

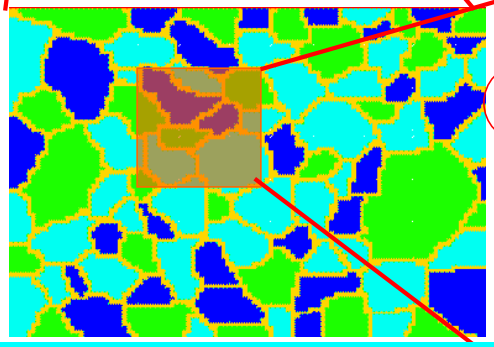

Finite Element Representation Based on Experimental Microstructural Characterization

Detailed View of Finite Element Mesh with Explicit GB and Orientation Representation

Propagation of Crack-Local View

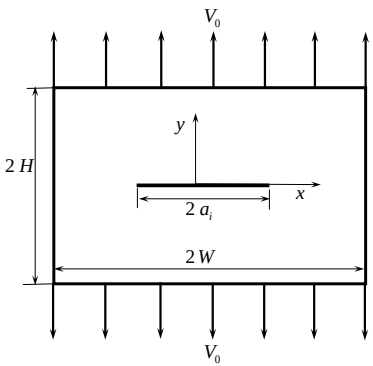

0.01312 µsec

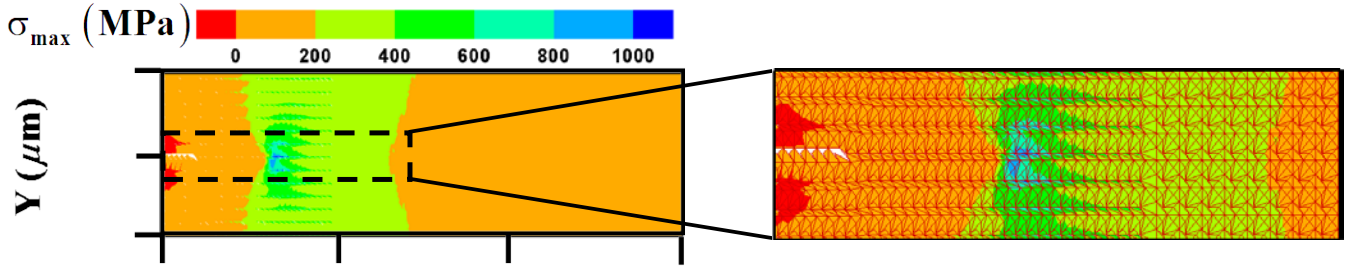

0.01688 µsec

(a)

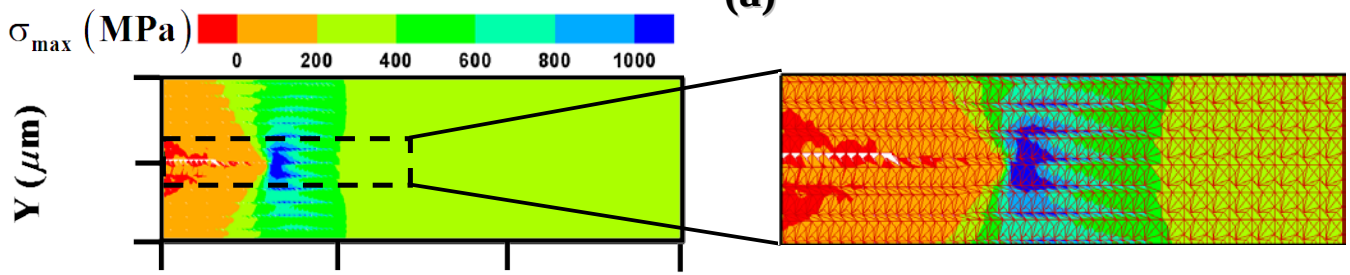

0.02437 µsec

(b)

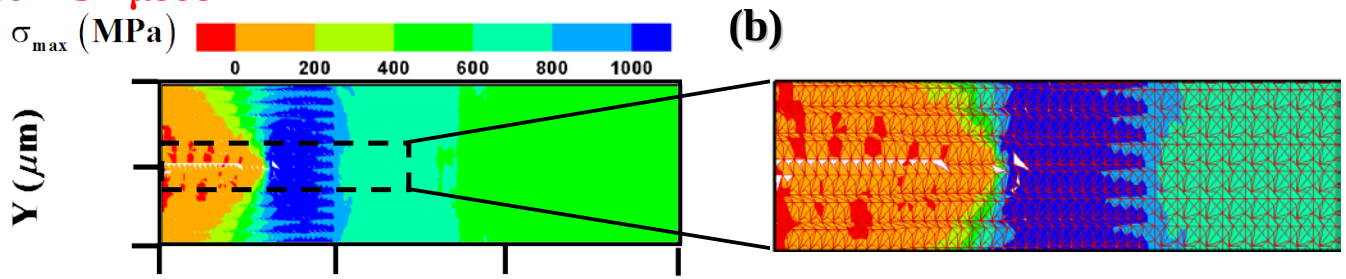

(c)

Microstructure Damage Pattern

$$D = \frac{\Phi_d}{\Phi_0},$$

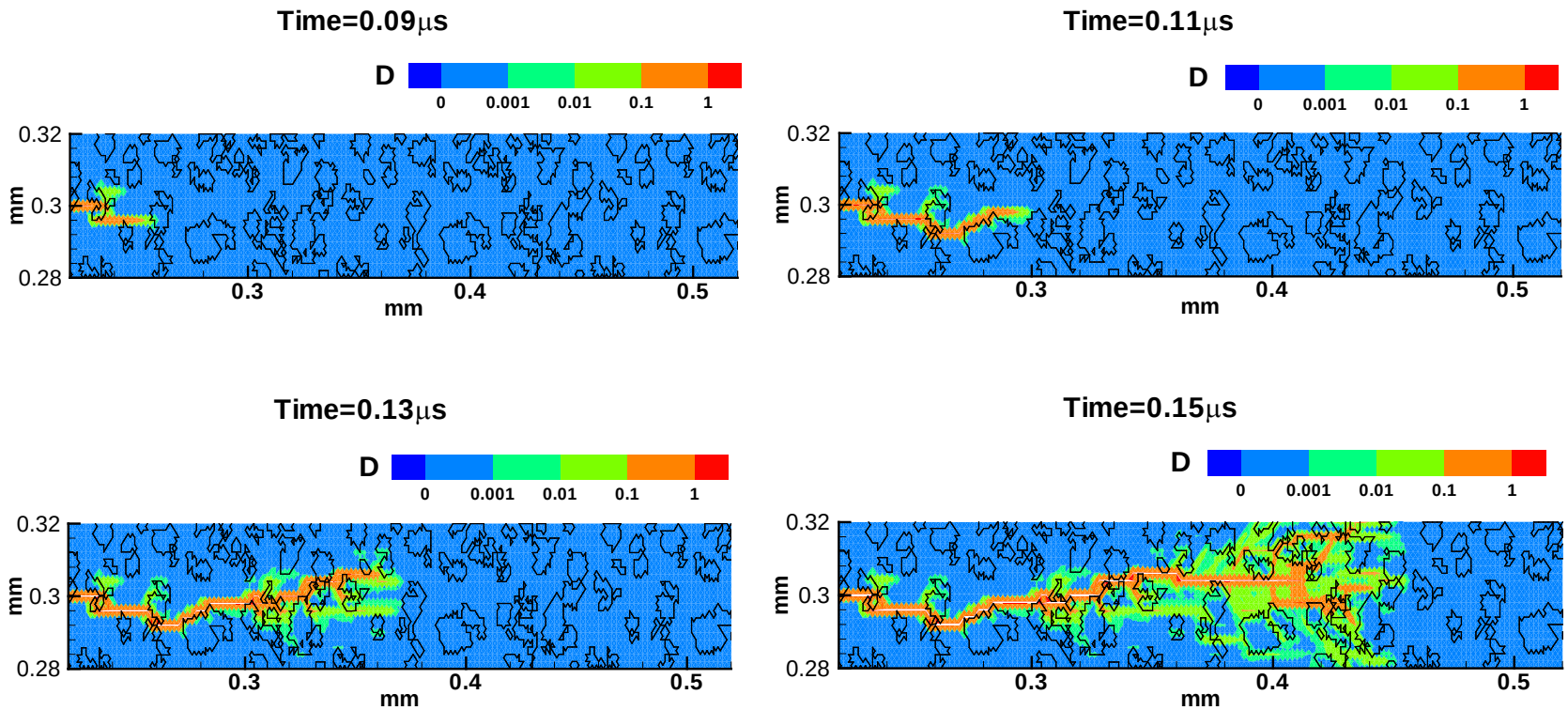

Propagation of Crack-Global View

Stress, [MPa]

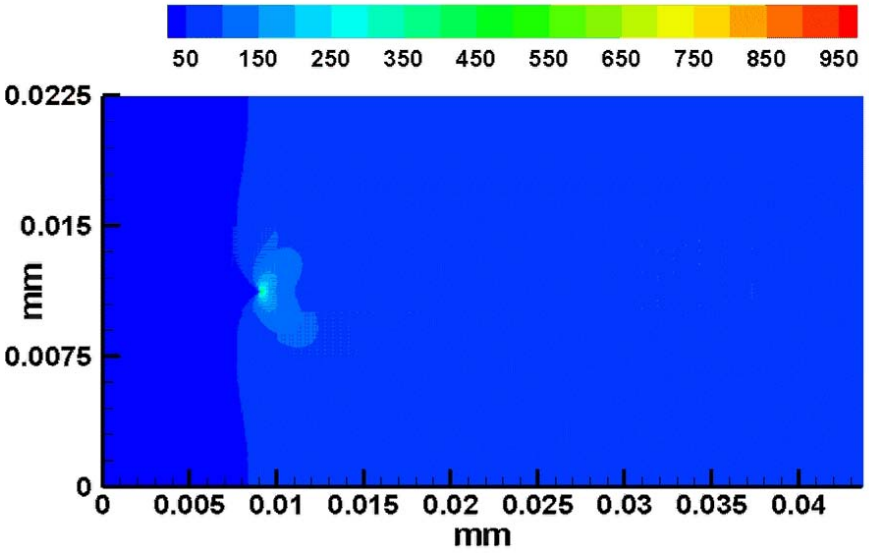

Damage $D = \frac{\Phi_d}{\Phi_0}, \quad 0 \le D \le 1$

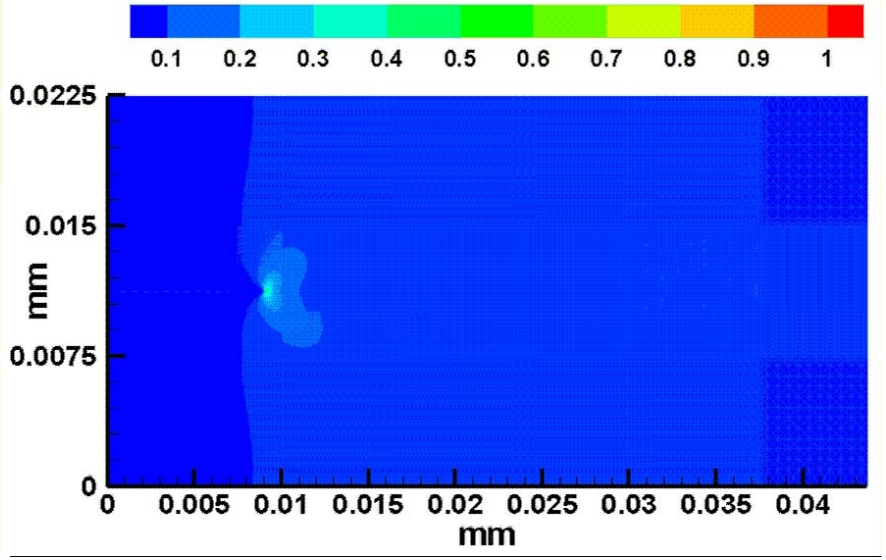

Microstructures of Focus-I

Class-I

SiC in Si_3N_4 matrix (InterST)

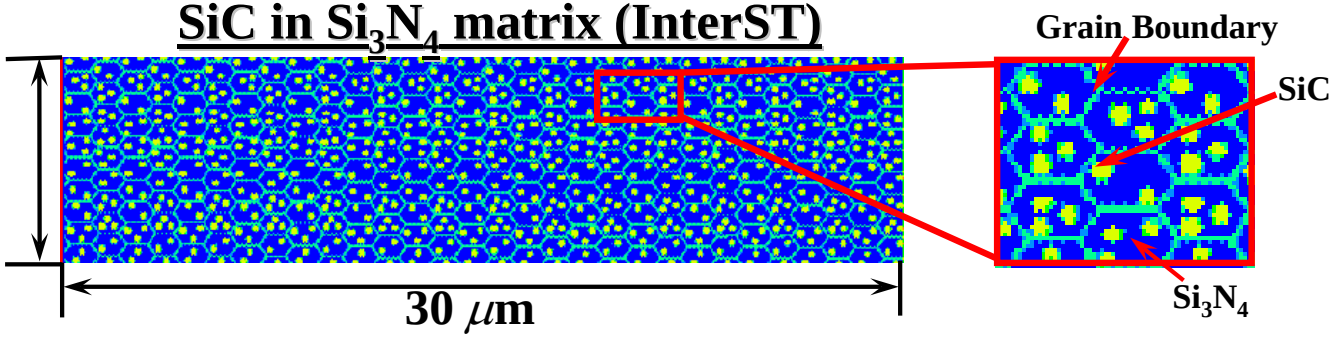

(a)

Class-II

SiC along GBs (IntraST)

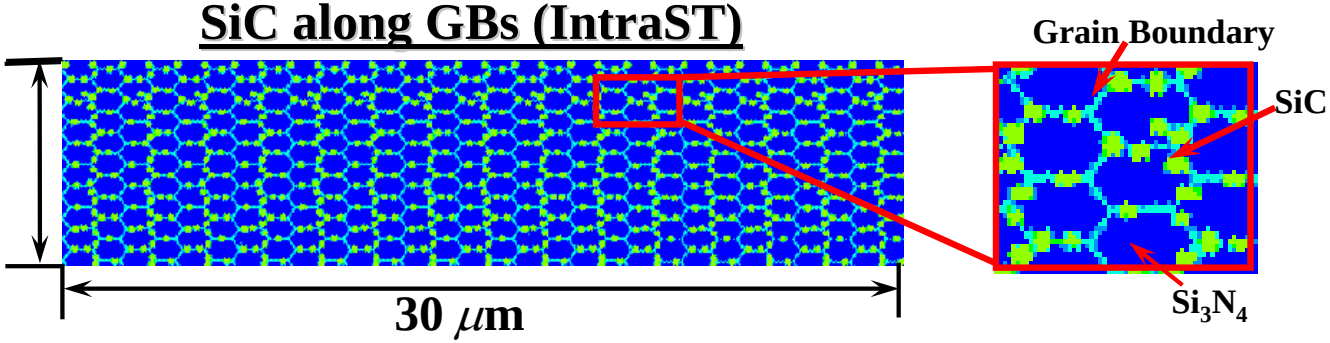

(b)

Class-III

SiC along GBs and in Si_3N_4 matrix (MixST)

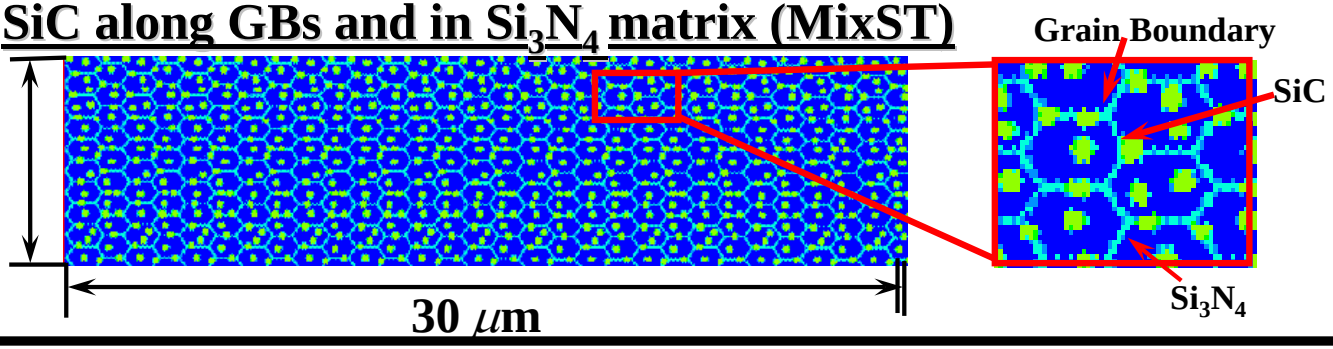

Damaging Effect of Second Phase Particles

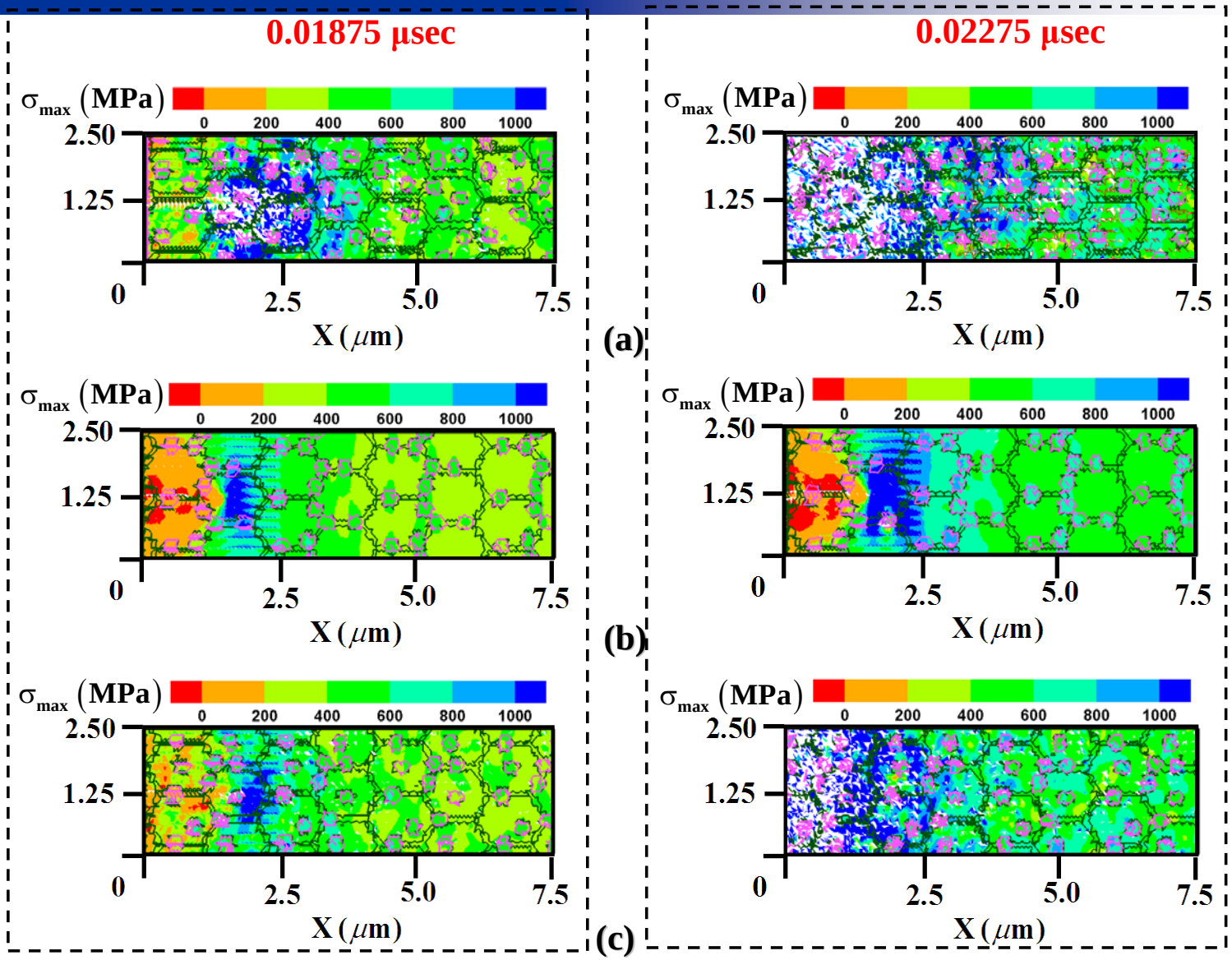

Microstructures of Focus-II

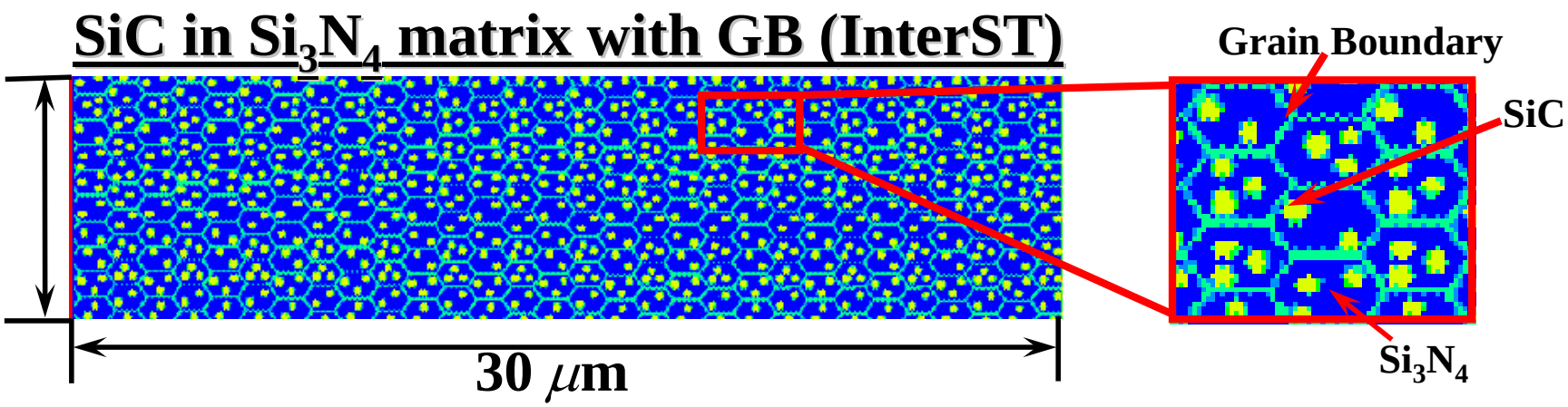

(a)

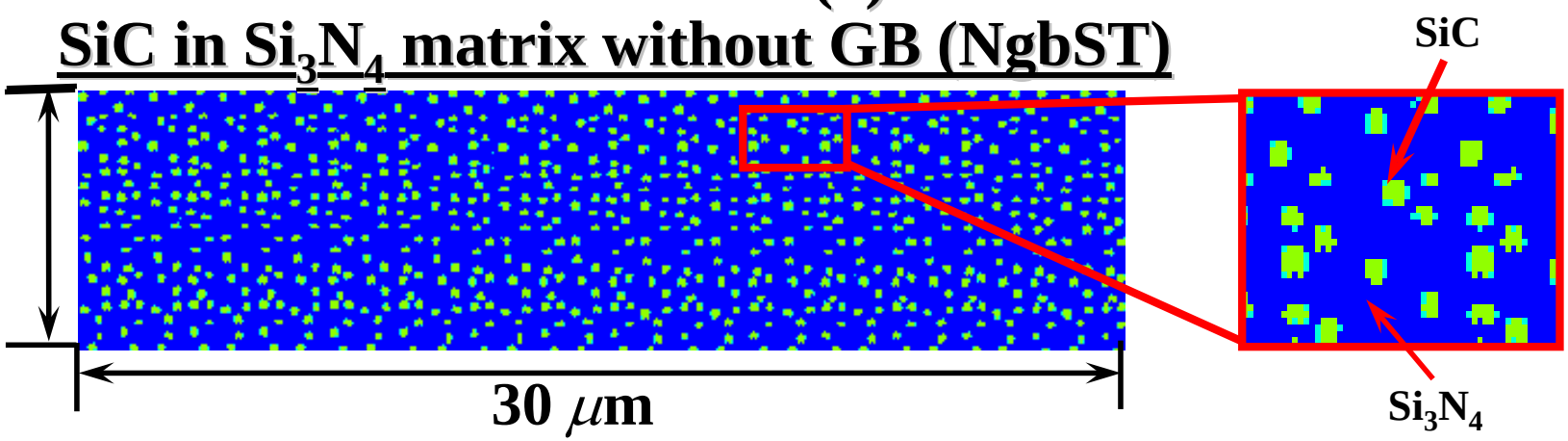

(b)

Damage Control Effect of GBs

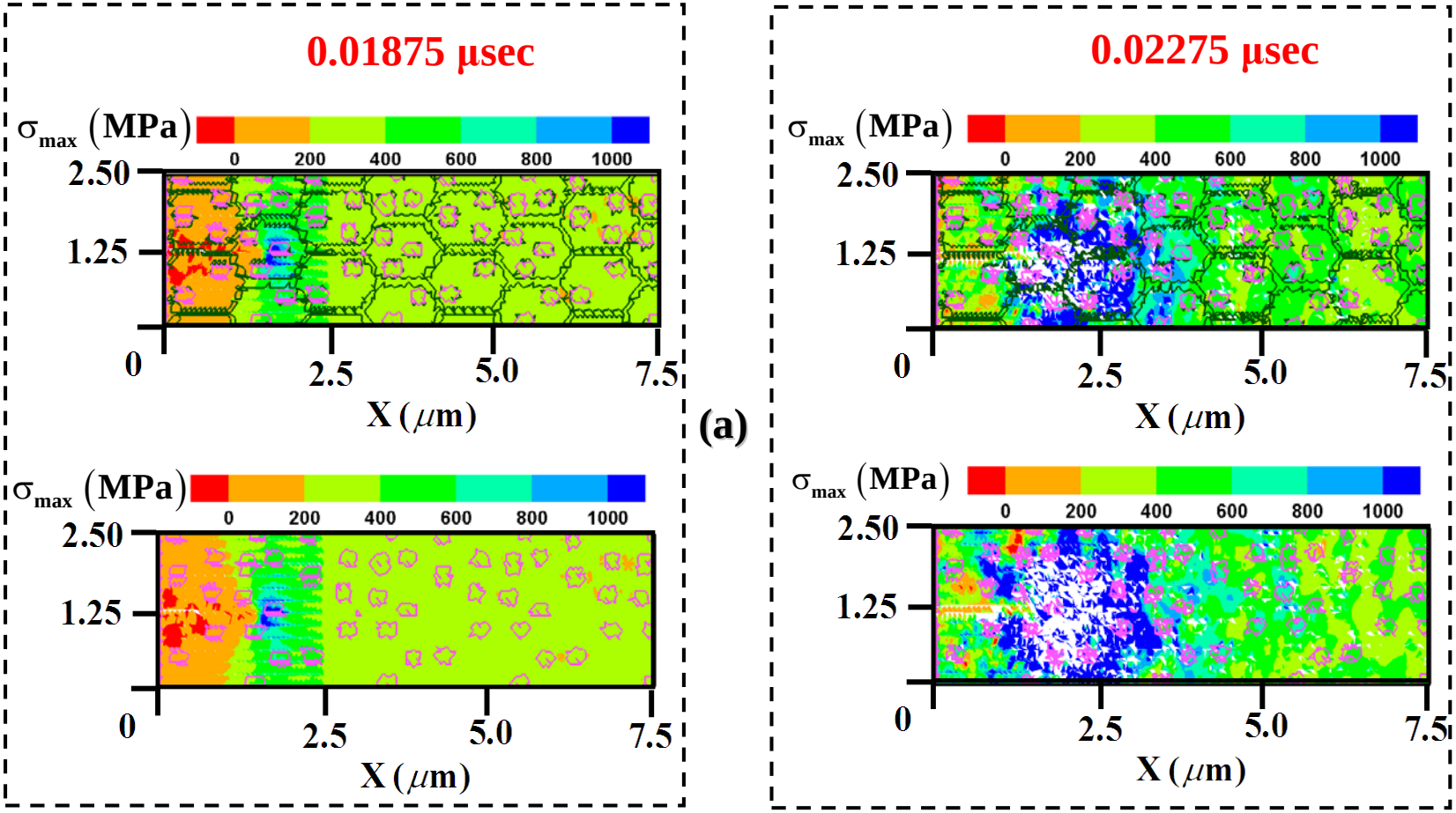

Outline

- High temperature creep and nanoindentation experiments in high temperature composites
  - Scale dependent nanoindentation upto 773 K
  - Nanoscale creep at different strain rates and maximum load
- Cohesive finite element based modeling of dynamic fracture failure in SiC-Si_3N_4 nanocomposites
  - Cohesive analyses accounting for second phase particle distribution and grain boundary distribution effects
  - High temperature constitutive models and trade-offs in designing these materials for high temperature performance
- **Insights from molecular analyses**
  - **Nanoscale fracture and strength at room temperature**
  - **Role of temperature in strength upto 1500 K**
- Designing materials in an optimization framework

Atomistic Microstructures To Analyze Particle Size Effect

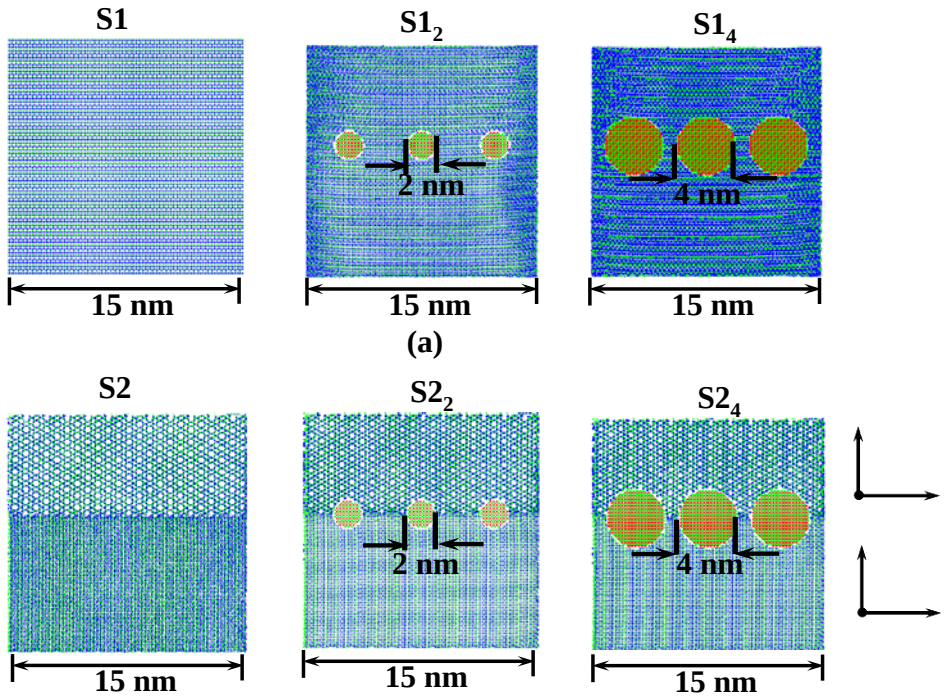

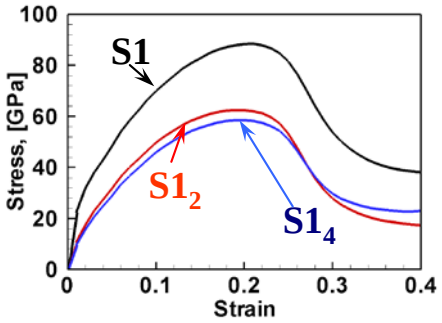

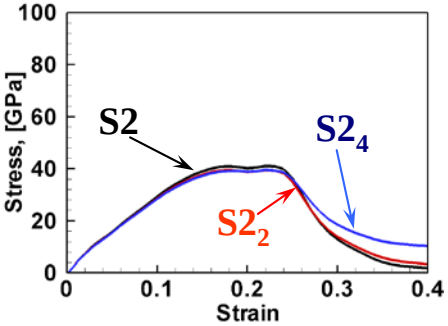

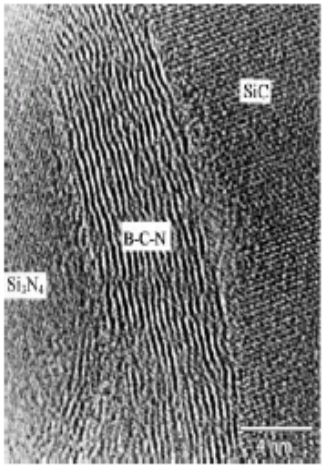

Particle Clustering

$S8_2$

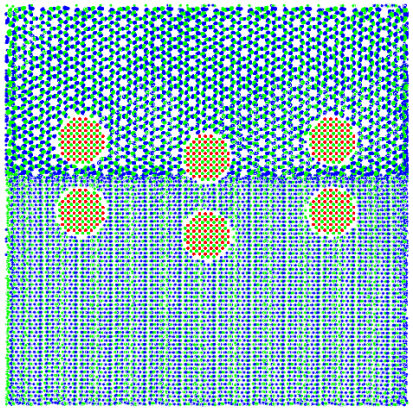

$S8_4$

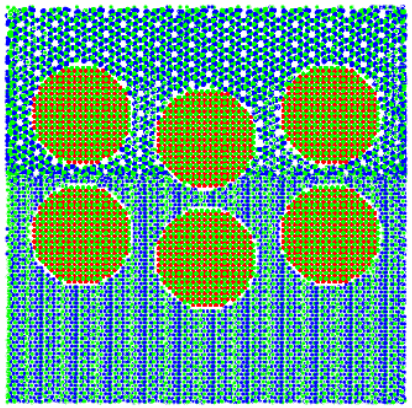

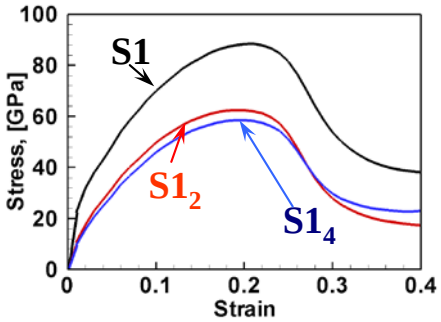

(a)

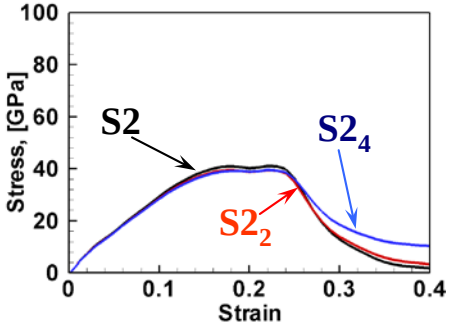

(b)

$S9_2$

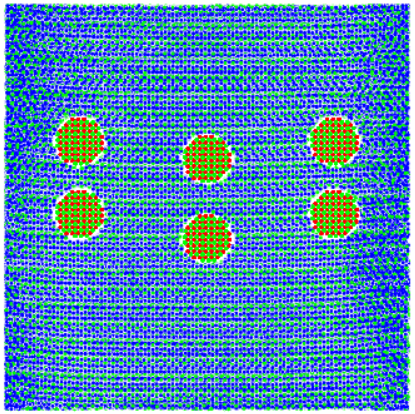

$S9_4$

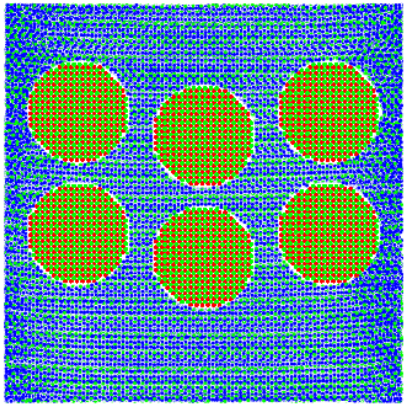

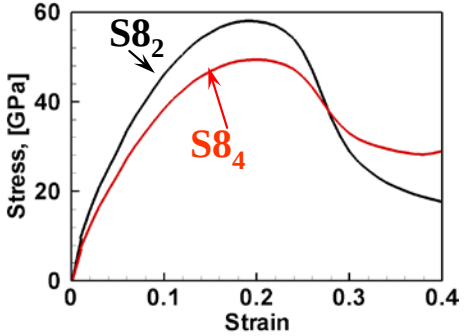

(a)

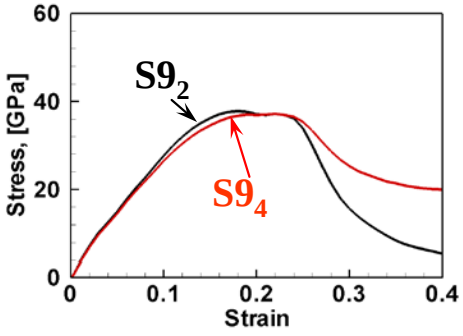

(b)

Microstructures Analyzed To Understand Effect of GB/Interface Thickness and Temperature

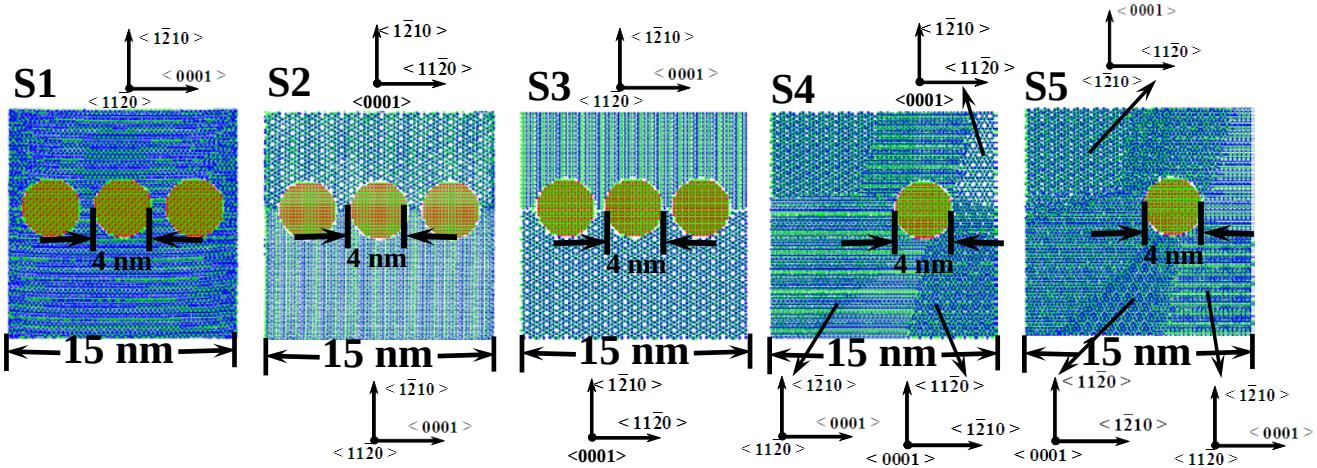

(a)

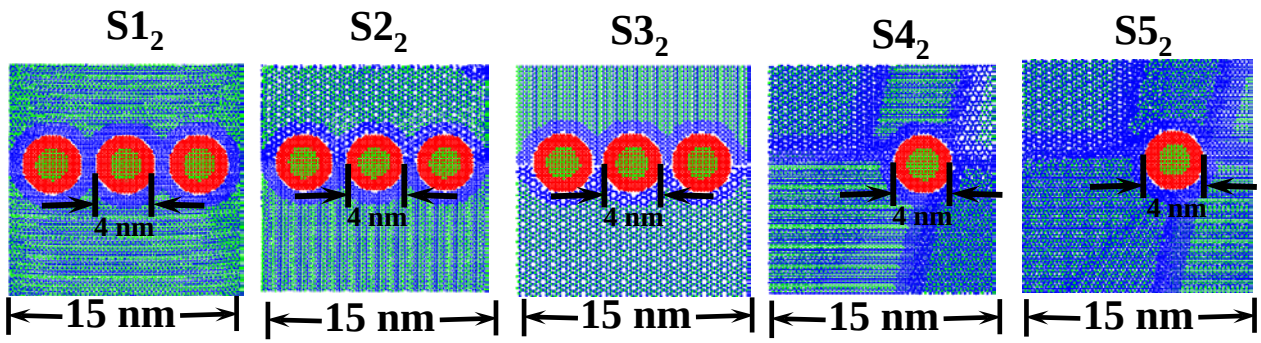

(b)

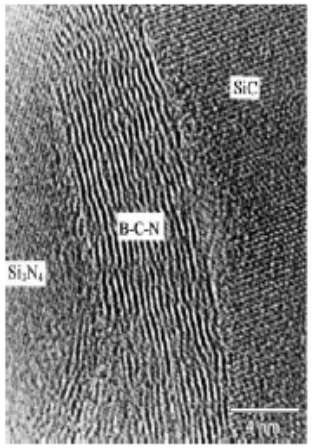

From R. Raj and co-workers

Stress-strain Relations

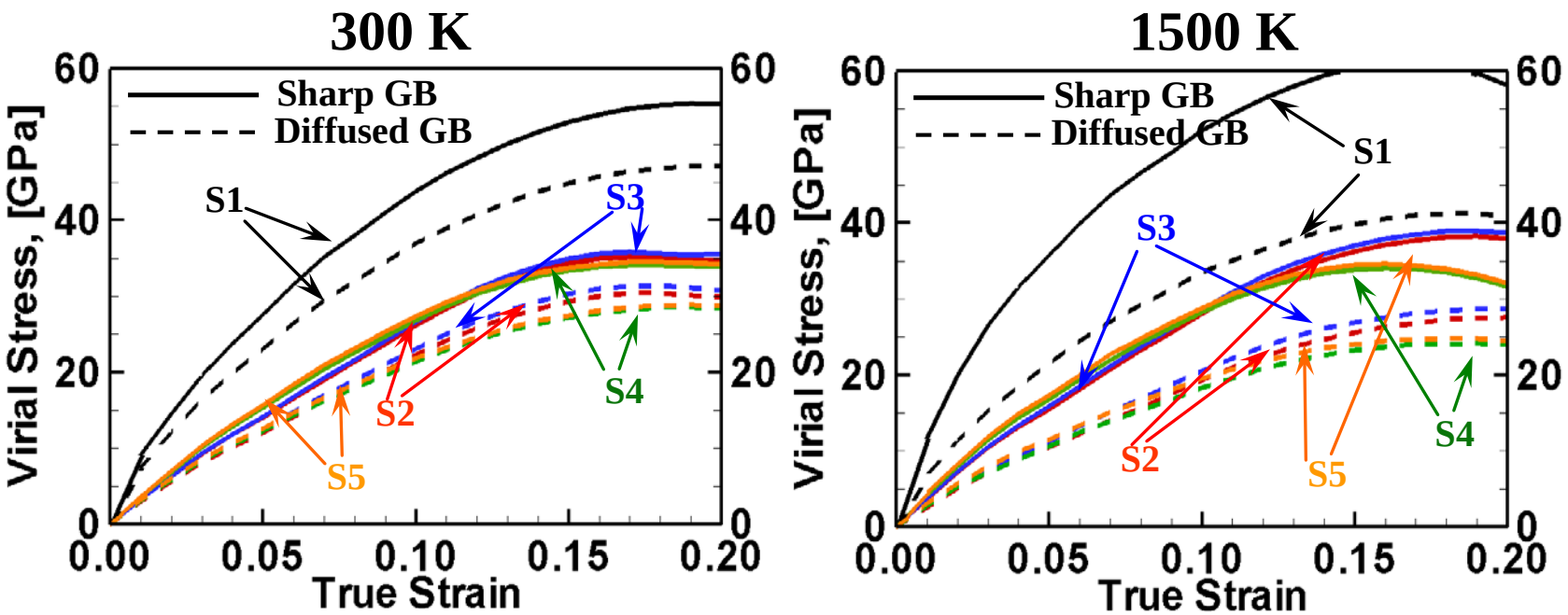

Effect of Temperature on Deformation Mechanism

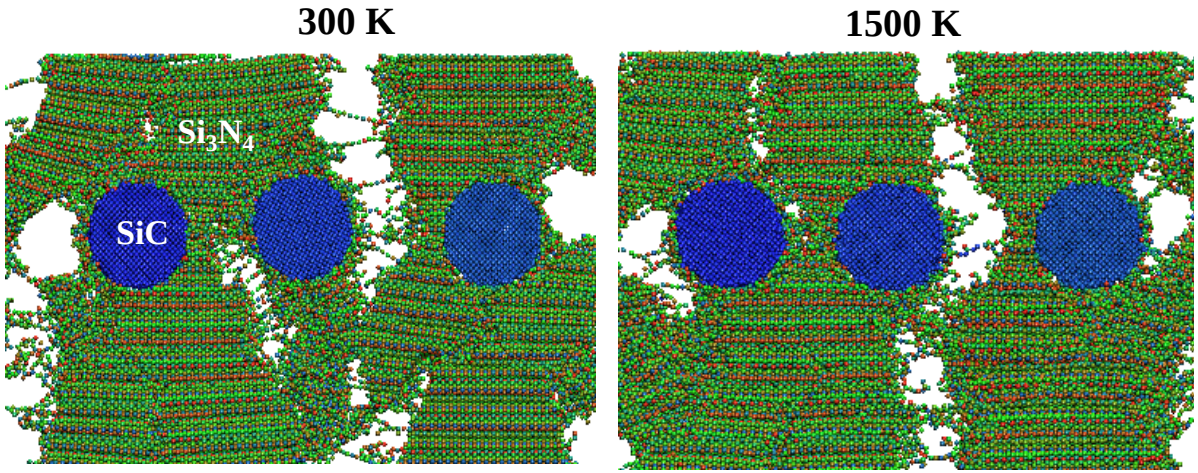

(a)

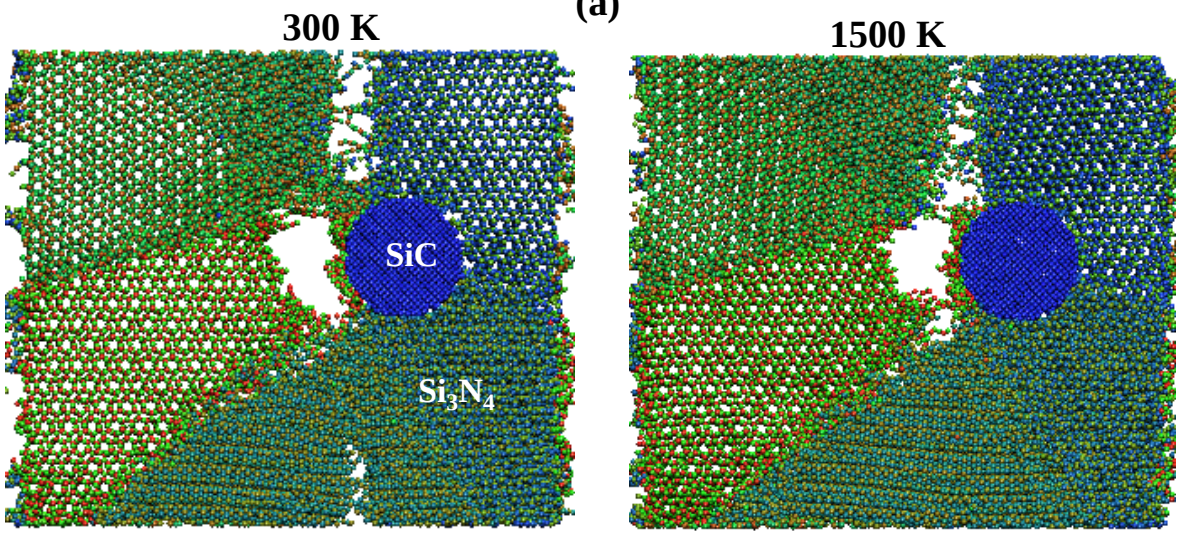

(b)

Outline

- High temperature creep and nanoindentation experiments in high temperature composites
  - Scale dependent nanoindentation upto 773 K
  - Nanoscale creep at different strain rates and maximum load
- Cohesive finite element based modeling of dynamic fracture failure in SiC-Si_3N_4 nanocomposites
  - Cohesive analyses accounting for second phase particle distribution and grain boundary distribution effects
  - High temperature constitutive models and trade-offs in designing these materials for high temperature performance
- Insights from molecular analyses
  - Nanoscale fracture and strength at room temperature
  - Role of temperature in strength upto 1500 K
- **Designing materials in an optimization framework**

Design Optimization

- Computer simulation can be very expensive for optimization.
- Need of optimization techniques for dealing with such simulations.

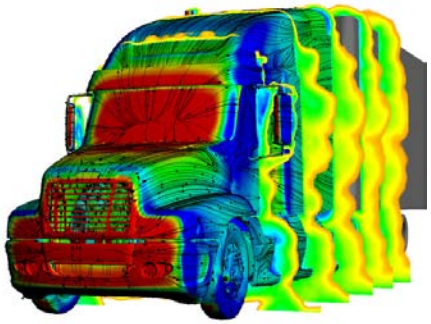

CFD

FEA

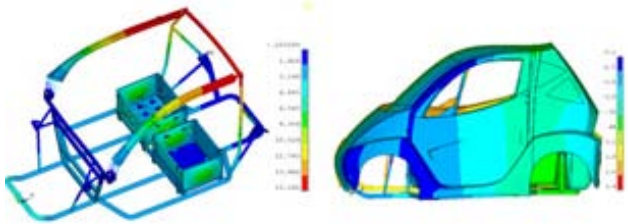

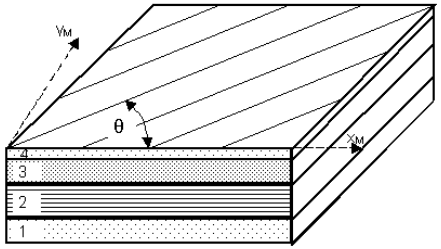

Layered Composites

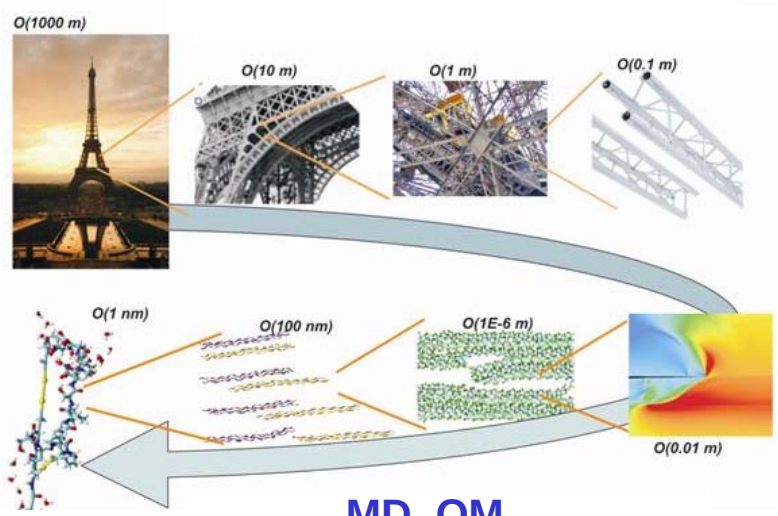

FEA

MD, QM

Computer-aided design to investigate materials for use in future high temperature power plant applications

Design Targets

Fracture and creep resistance at about 1800 K

$SiC-Si_3N_4$

Design Variables

- Phase size
- Phase Volume Fraction

Variable Fidelity Optimization

Multiscale Material Simulation

Optimal Morphologies

$SiC-Si_3N_4$ nanocomposite with desired properties

Want: Accuracy of quantum mechanics (QM) in 10^{23} atom systems…

This is impossible (today and in the foreseeable future)

Possible solution:
Multi-scale modeling techniques based on hierarchies of overlapping scales

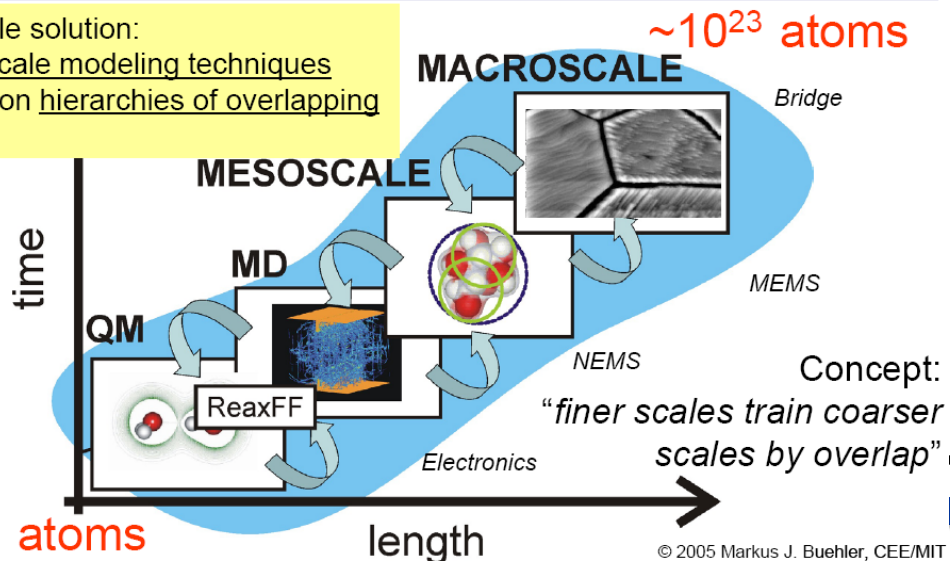

Concept:
"finer scales train coarser scales by overlap"

© 2005 Markus J. Buehler, CEE/MIT

Material Design Methodology

- Address computational challenges.

- Address model management issues.

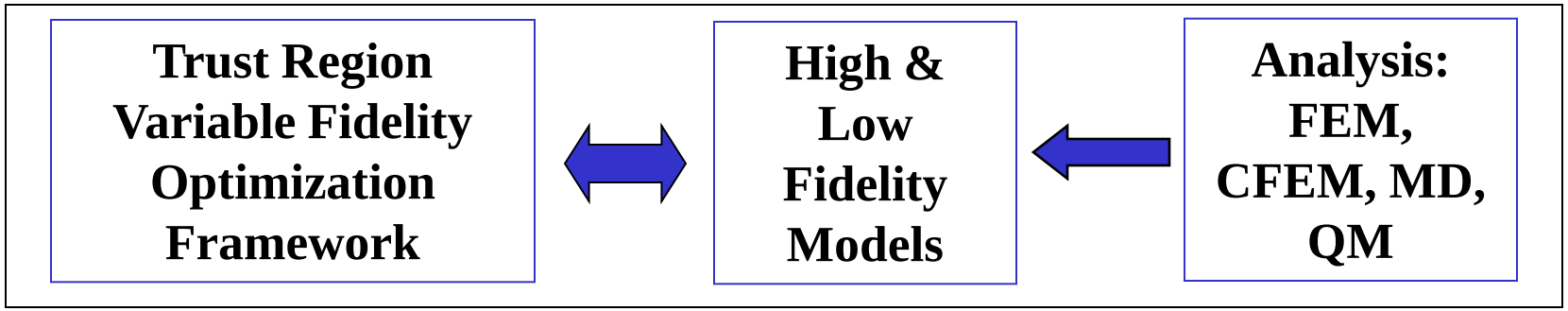

Design Targets
Design Variables

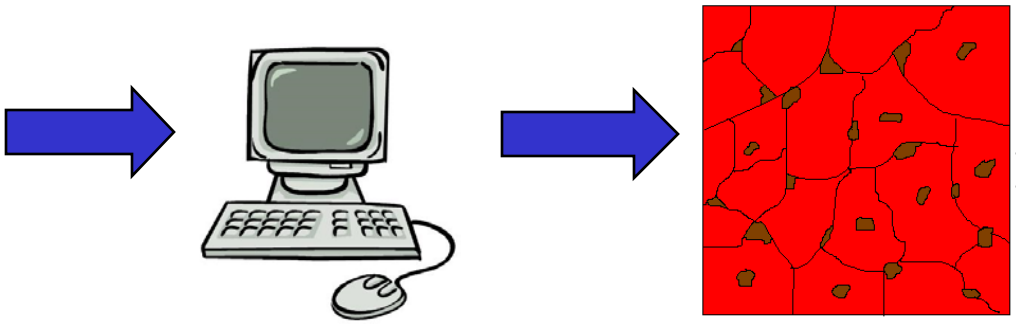

Optimal Morphology

Objectives: Definition of Models

LOW FM		HIGH FM
PROBLEM 1 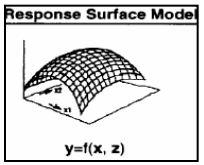 $K_I = \frac{PS}{BW^{3/2}} f\left(\frac{a}{W}\right)$ Analytical Fracture Mechanics & Surrogate Modeling	Fracture toughness	FEM (Comsol) 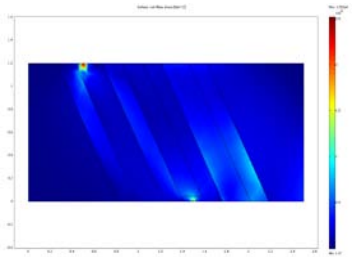
PROBLEM 2 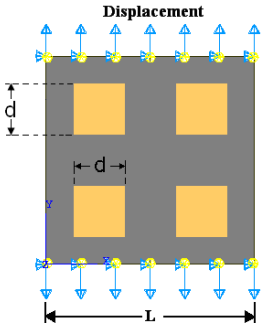 FEM (ABAQUS) 2D Model	Strength & Creep strain resistance	FEM (ABAQUS) 3D Model 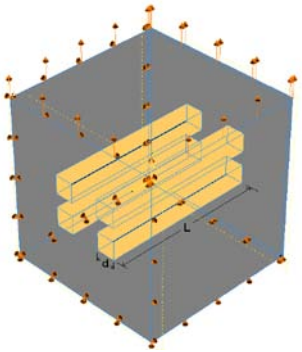
PROBLEM 3 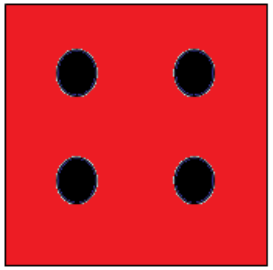 FEM (ABAQUS) Ideal microstructure	Strength & Creep strain resistance	CFEM (ABAQUS) Real microstructure 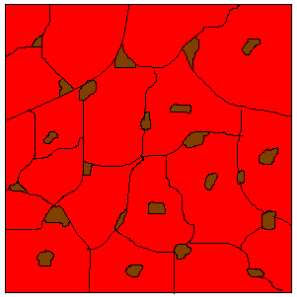

Variable Fidelity Optimization Algorithm

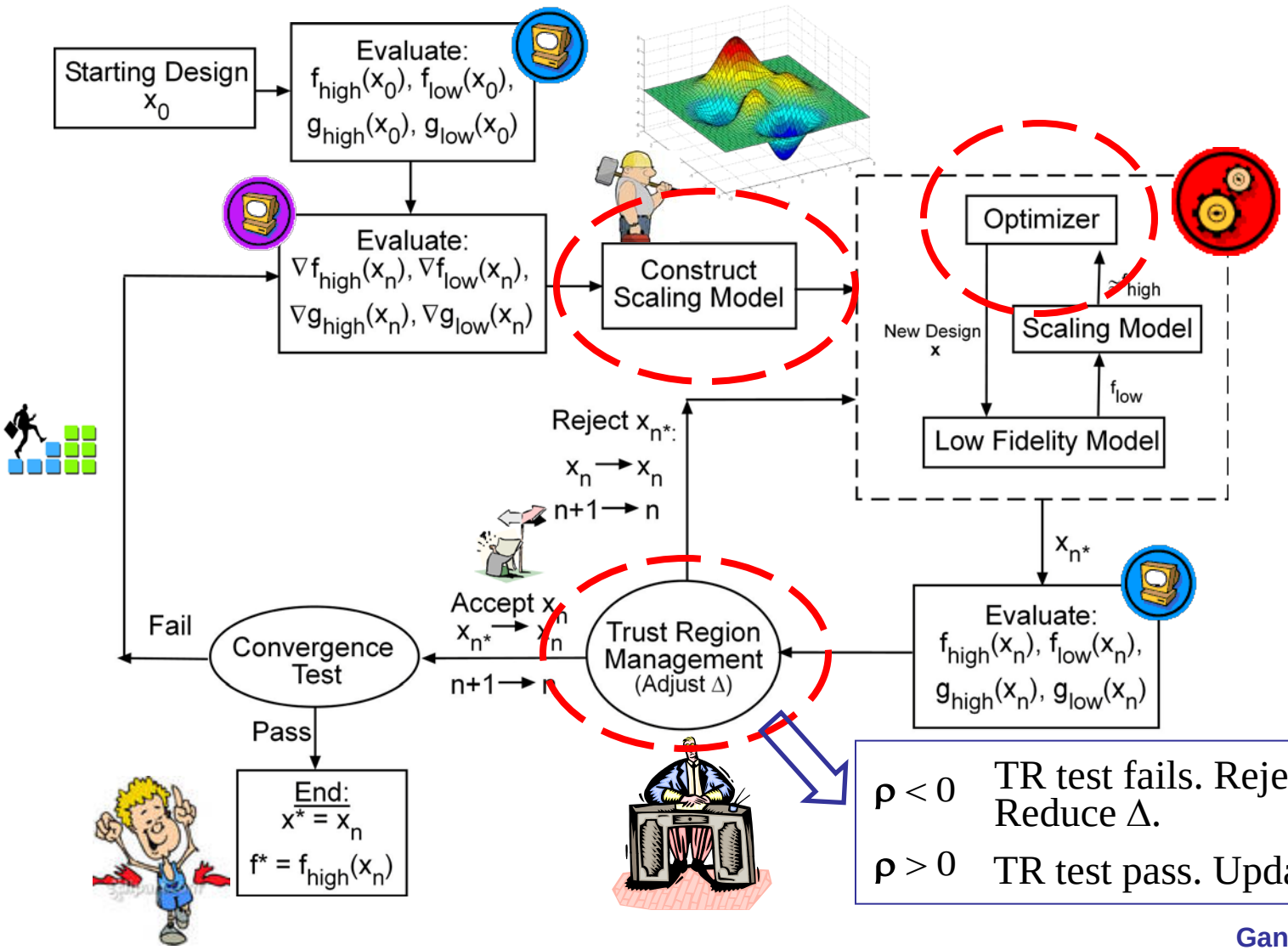

$\rho < 0$	TR test fails. Reject step. Reduce Δ.
$\rho > 0$	TR test pass. Update Δ.

Gano *et al.*, 2004

Problem 1

Find optimal CFCC configuration for improving fracture toughness (K_{IC})

Construct scaling model

$$\beta(x) = \frac{f_{high}(x)}{f_{low}(x)} \Rightarrow f_{high}(x) \approx \beta(x) f_{low}(x)$$

Optimize scaling model

$$\begin{aligned} &\text{maximize} && \beta_n^1 K_{IC_{LOW}}(V_f, \theta), \\ &\text{subject to:} && \beta_n^2 K_{I_{LOW}} \le \beta_n^1 K_{IC_{LOW}}(V_f, \theta), \\ & && 0 \le V_f \le 0.2, \\ & && 0° \le \theta \le 90°, \\ & && -0.05 \le \Delta V_f \le 0.05, \text{ and} \\ & && -4° \le \Delta\theta \le 4° \end{aligned}$$

Design Target

Fracture resistance

Variable Fidelity Optimization

Simulations

Optimal Morphology

Design Variables

- Second Phase orientation angle θ
- Second Phase Volume Fraction

$$\begin{aligned} &\text{maximize Mode-I } K_{IC}(V_f, \theta) \\ &\text{subject to:} \quad K_I \le K_{IC}(V_f, \theta) \\ &\qquad 0 \le V_f \le 0.2 \\ &\qquad 0° \le \theta \le 90° \end{aligned}$$

Design load 93500 N → K_I

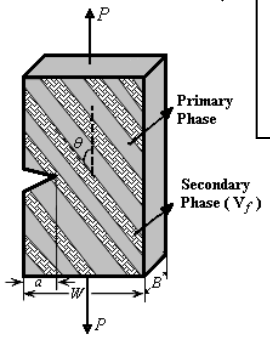

High fidelity (HF) model

K_{IC} and K_I obtained using FEM (COMSOL)

Low fidelity (LF) model

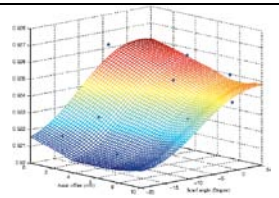

Response surface approximation for K_{IC}

$$K_I = \frac{PS}{BW^{3/2}} f\left(\frac{a}{W}\right)$$

Analytical fracture mechanics for K_I

Mejia-Rodriguez, G., J.E. Renaud, and V. Tomar, *A variable fidelity model management framework for designing multiphase materials.* Journal Of Mechanical Design, 2008. 130(9).

Results

- Initial design: V_f^0 = 0.05, θ^0 = 0.3 rad
- K_{IC}^0 = 7013519.6 MPa·m$^{1/2}$

80% reduction in HF simulations

Optimization Method	Low Fidelity Simulations	High Fidelity Simulations	Iteration	θ^*(rad.)	V^*_f	K_{IC}^*(MPa·m$^{1/2}$)
Conventional	0	109	10	0.08528	0.2	7239246.361
Variable Fidelity	187	24	4	0.08531	0.2	7239245.175

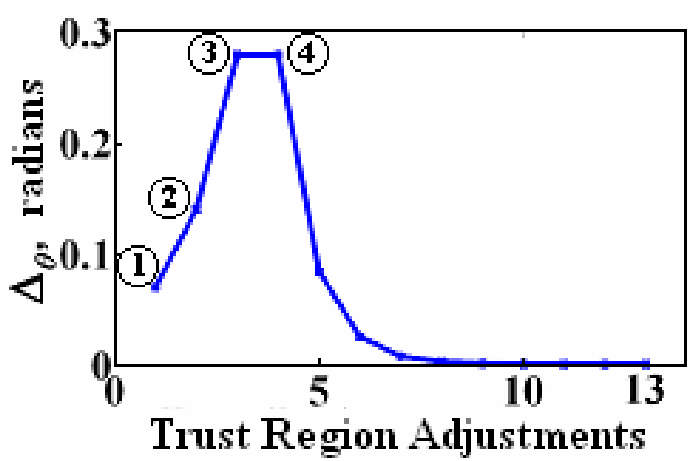

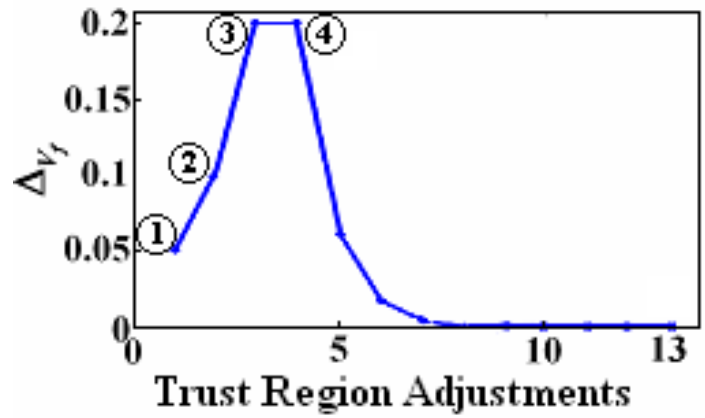

Iteration	Trust Region Adjustments	Trust Region Size		Convergence		Design Varibles and Obj. Function		
		$\Delta\theta$	ΔV_f	Δ_x	Δ_f	θ(rad.)	V_f	K_{IC} (MPa·m$^{1/2}$)
1	1	0.07	0.05	0.2828	0.0111	0.23	0.1	7091470.873
2	1	0.14	0.10	0.6859	0.0208	0.09	0.2	7239211.263
3	1	0.28	0.20	0.0214	4E-06	0.08530	0.2	7239241.029
4	10	2.1E-10	0.0000012	0.00002	6E-07	0.08531	0.2	7239245.175

Problem 2

Find optimal CMC (ceramic matrix composite) configuration

- Incorporate Multiobjective Optimization formulation
- Construct scaling model: It will allow to incorporate higher dimensionality that is not present in LF model

Design Target

Strength & Creep resistance

Variable Fidelity Optimization

Simulations

Pareto Optimal Morphology

Ideal microstructures

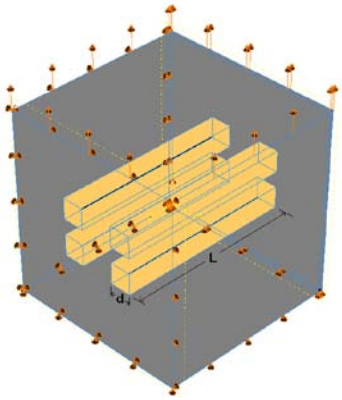

3-D HF FEA model

Design Variables

***d*-Grain width-height**

***l*- Grain length**

***T*-Temperature**

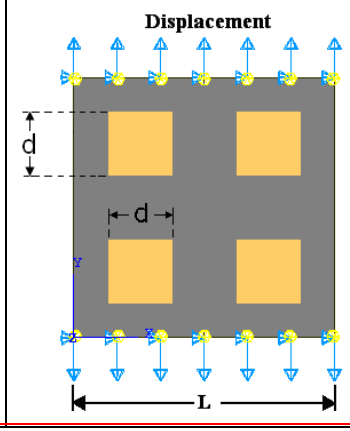

2-D LF FEA model

Design Variables

***d*-Grain width-height**

***T*-Temperature**

Continuum based models are used to define:

- Flow stress
- Creep strain rate

- **Multiphysics models with different input variables**
- **2D LF captures physics of 3D HF**

Creep Model for SiC (Hexology)

➢**By using the Norton relation for stress, the secondary creep relation for time and the temperature dependence, the creep strain rate expression for SiC used in this research takes the form:**

$$\dot{\varepsilon}_c = A\sigma^n \exp\left(-\frac{Q}{RT}\right)$$

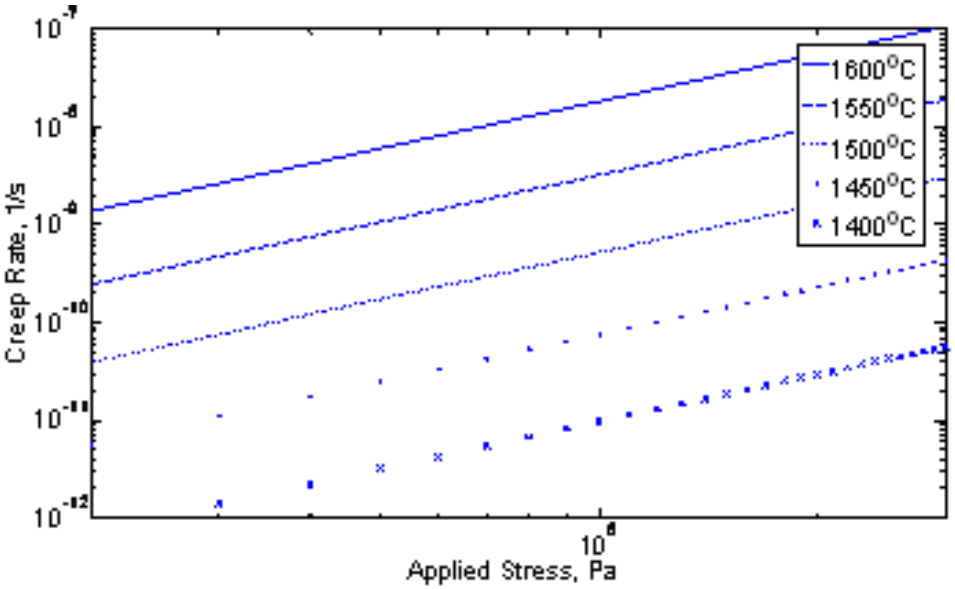

A fit to tensile data collected on Hexology

Wiederhorn et al., 1999

The constants *A*, *Q* and *n* are determined from a fit of the last equation to experimental data taken at 150 MPa and at temperatures ranging from 1500 C to 1600 C.

***A* = 6.2e6 seg.$^{-1}$Pa^{-1}**

***n* = 1.6**

***Q* = 980 KJ/mol**

***R* = 8.31447 J/mol K**

Creep Model for Si_3N_4 (SN-88)

The creep strain rate the creep strain rate expression for Si3N4 used in this research takes the form:

Krause R.F. et al., 1999

$$\dot{\varepsilon}_c = A\sigma \exp(\alpha\sigma)\exp\left(-\frac{Q}{RT}\right)$$

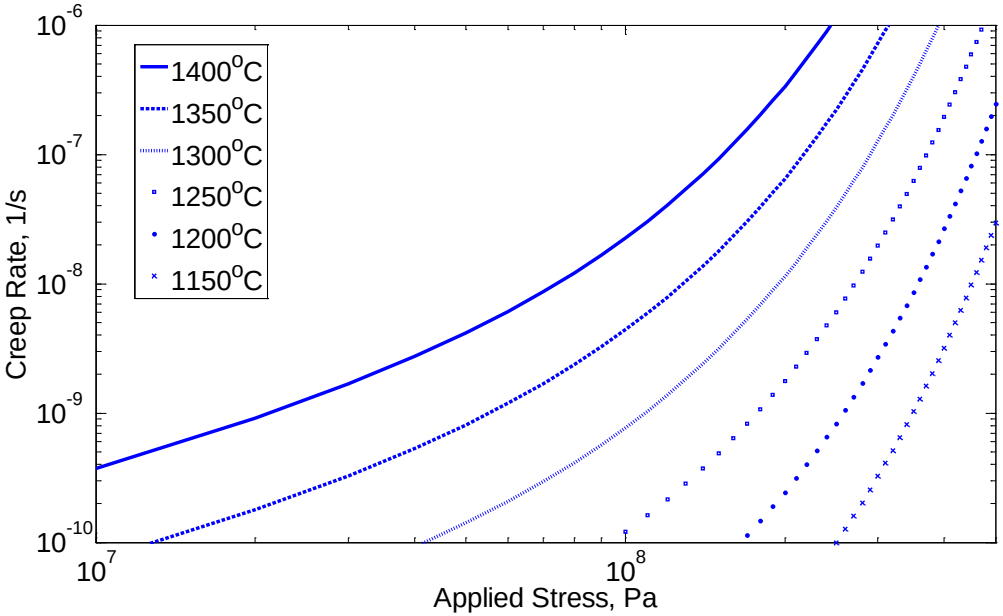

The constants *A*, *Q*, and α are determined from a fit of the last equation to experimental data taken at 1150 C, 1200 C, 1250 C, 1300 C, 1350 C and 1400 C; and at stresses ranging from 10 to 400 MPa.

A = 3.89e6 seg^{-1}

α = 0.0197 0.0008 MPa-1

Q = 715.3 22.9 KJ/mol

R = 8.31447 J/mol K (Boltzmann's constant)

Fit of tensile data collected on SN-88 *Yoon et al., 2000*

Stress-Strain curves

❖Yield function for strength (Si_3N_4 & SiC)

$$\sigma = \sigma_0 \left[1 + \left(\frac{\varepsilon}{\varepsilon_0} \right)^n \right] \left[\frac{\dot{\varepsilon}}{\dot{\varepsilon}_0} \cdot \exp\left(\frac{Q}{RT} \right) \right]^m$$

Lei et al., 2000

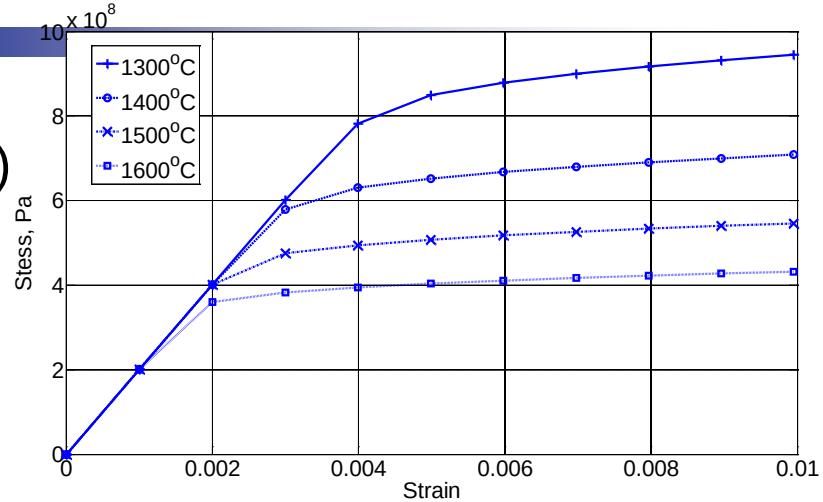

Stress-Strain curve for Si_3N_4 showing increment in strength as temperature goes down from 1600°C to 1300°C.

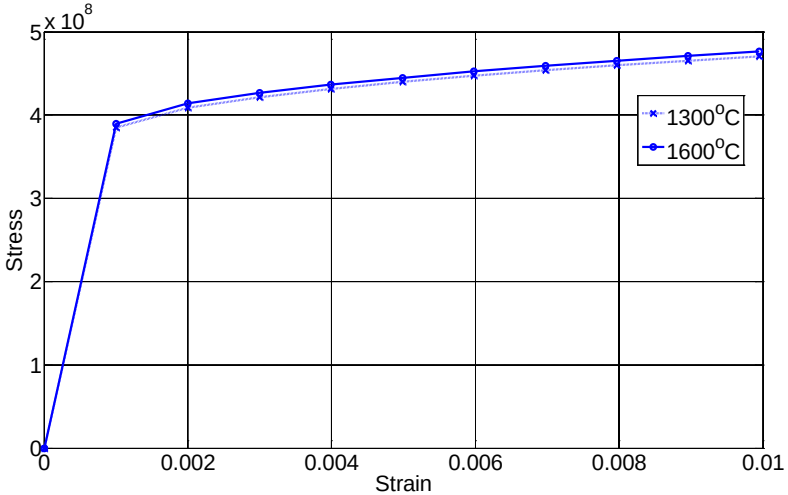

Stress-Strain curve for SiC showing small increment in strength as temperature rises from 1300°C to 1600°C.

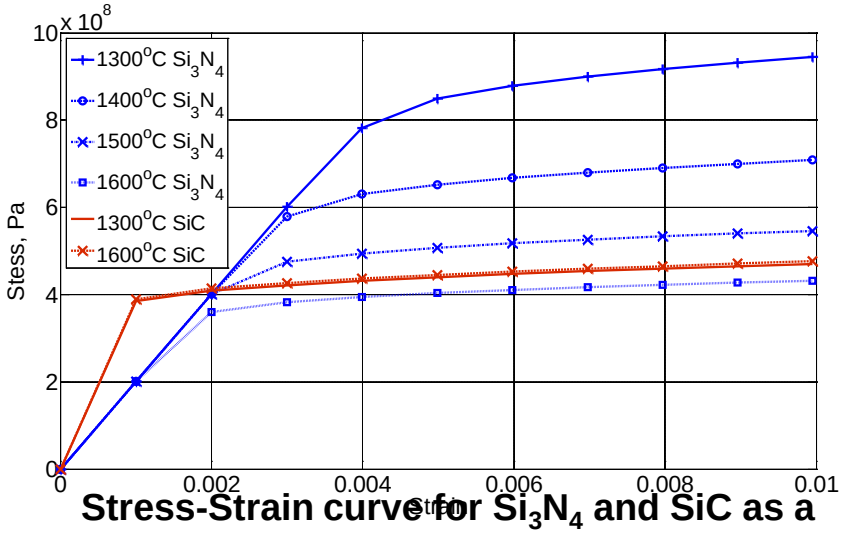

Stress-Strain curve for Si_3N_4 and SiC as a function of temperature.

Strength and Creep behavior as a function of Design Variables

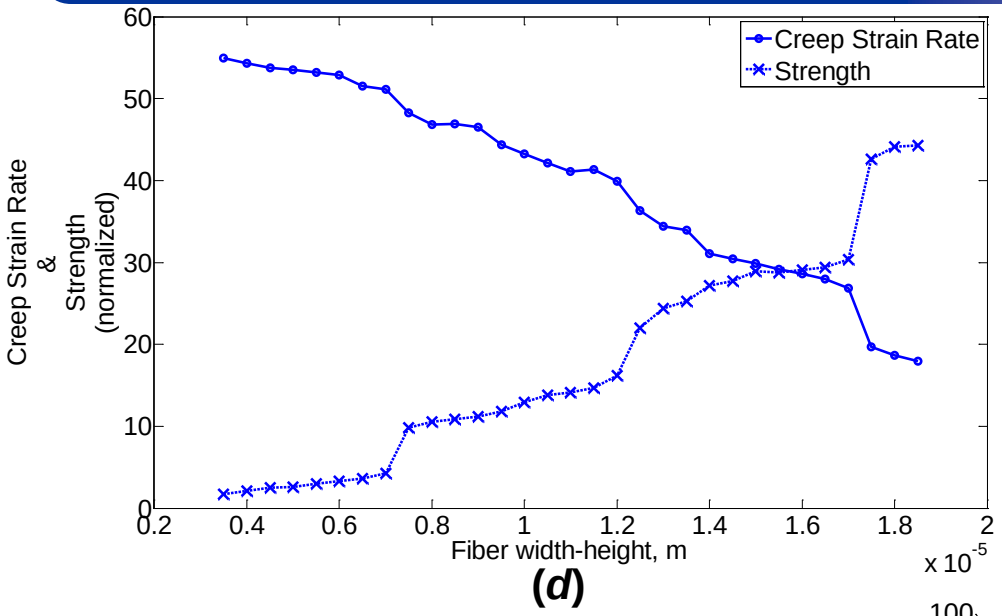

Strength and creep strain rate at 1500°C as a function of the design variable fiber width-height (*d*) for the 2-D low fidelity model.

Strength and creep strain rate at 1500°C as a function of the design variables fiber width-height (*d*) and fiber length (*l*) for the 3-D high fidelity model.

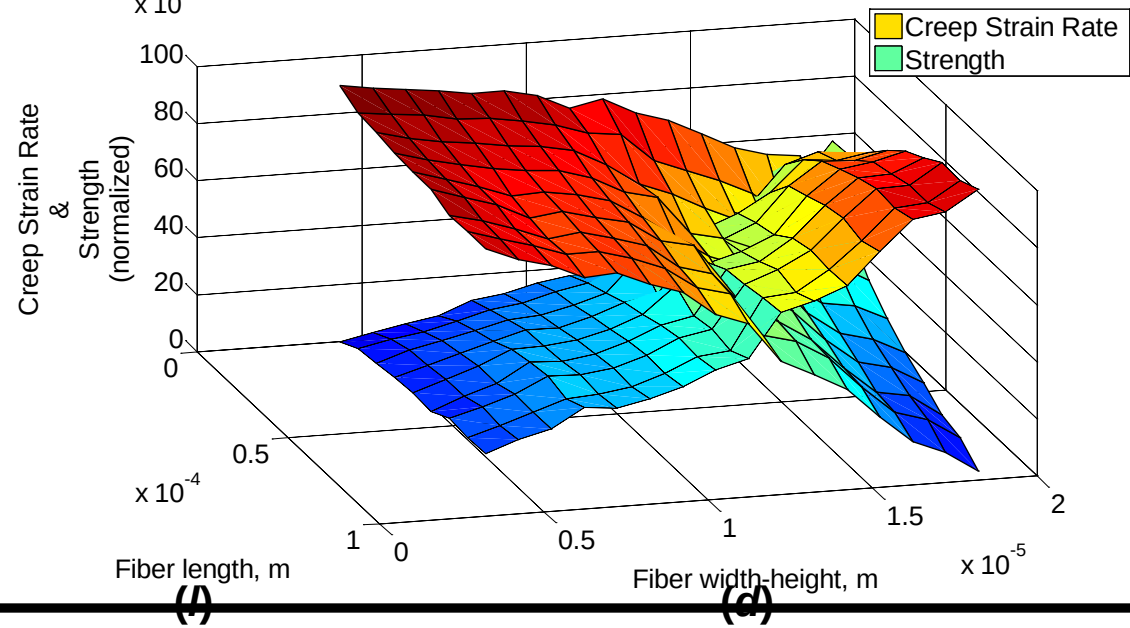

Problem 3

Develop nanocomposites whose performance variation is insensitive to processing (microstructure) variations

- **Incorporate Multiobjective Optimization formulation**
- **Incorporate Robust Optimization approach.**
- **Construct scaling model**

Design Targets

- Fracture Toughness
- Strength
- Creep resistance

Variable Fidelity Optimization

Simulations

Pareto Optimal Morphology

- **Multiphysics models with different input variables**
- **LF captures physics of HF**

HF real microstructure

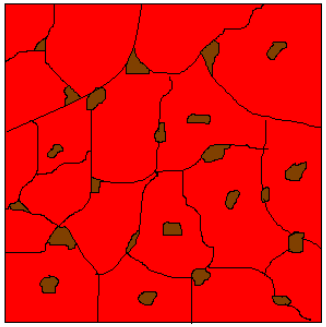

Design variables

- Grain size distribution
- Number of grains
- Volume fraction
- Grain orientation

CZM at grain boundaries & continuum models to define behavior of single phase

LF ideal microstructure

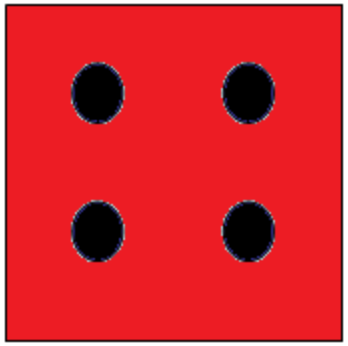

Design variables:

- Grain size
- Number of grains
- Volume fraction

Elasto-plastic continuum models to define behavior of single phases

Microstructural Postprocessing

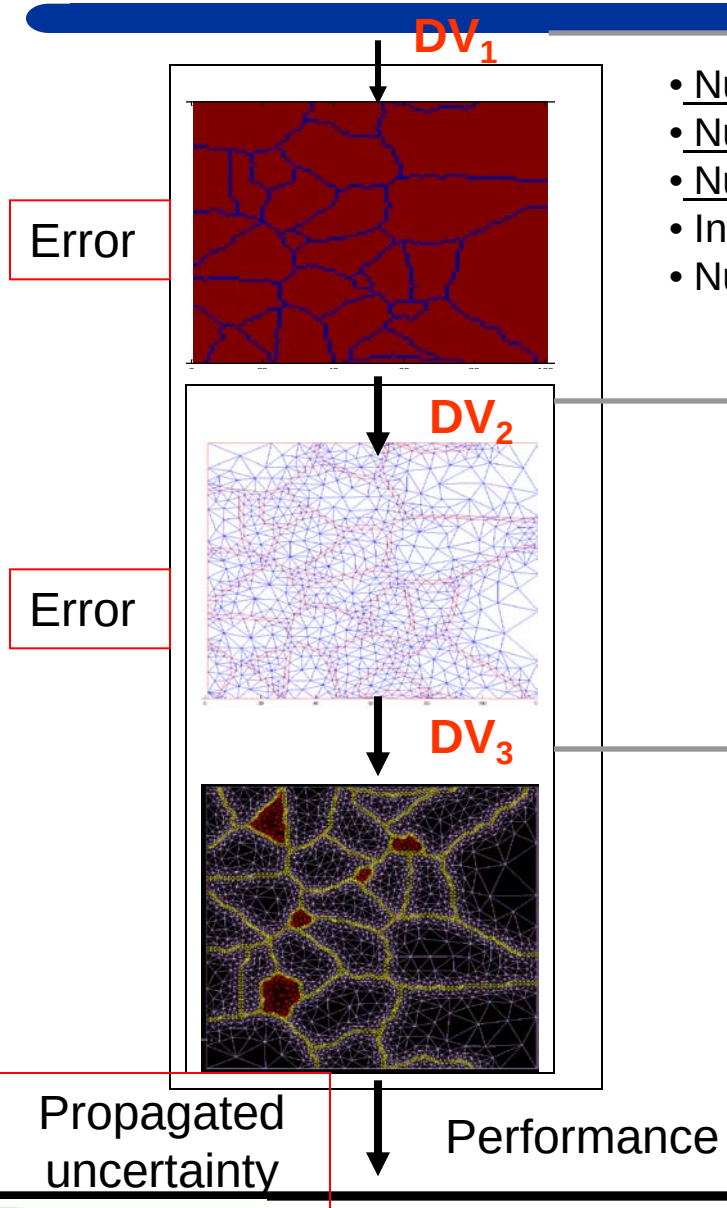

- Number of Si_3N_4 grains
- Number of Intergranular SiC grains
- Number of Intragranular SiC grains
- Initial nucleation (Si_3N_4 grains)
- Nucleation rate (Si_3N_4 grains)

- Growth of Intergranular SiC grains
- Growth of Intragranular SiC grains

- Volume fraction
- Grains size
- Grain size distribution
- Number of grains

- Volume fraction
- Grains size
- Grain size distribution
- Number of grains

Submitted to AIAA J, 2010

Microstructure size: 100μm x 150μm

Optimization Formulation

$$\text{Minimize} \quad S_r = \alpha \cdot [-\bar{S}_r] + (1-\alpha) \cdot vrt[S_r]$$

α = 1 and α = 0.5, at T=1500°C and T=1600°C

4 cases

$$\text{Minimize} \quad S_{r_mo} = w_1 S_r(\alpha, \text{T=1500}) + w_2 S_r(\alpha, \text{T=1600})$$

α = 1 and α = 0.5 (w_1=w_2=0.5)

2 cases

Quadratic least square response surface

$$\tilde{T}(z) = a_0 + \sum_{i=1}^{n} a_i z_i + \sum_{i=1}^{n} \sum_{j=1}^{n} a_{ij} z_i z_j$$

Fractional factorial design sampling

(get μ and σ for each sample)

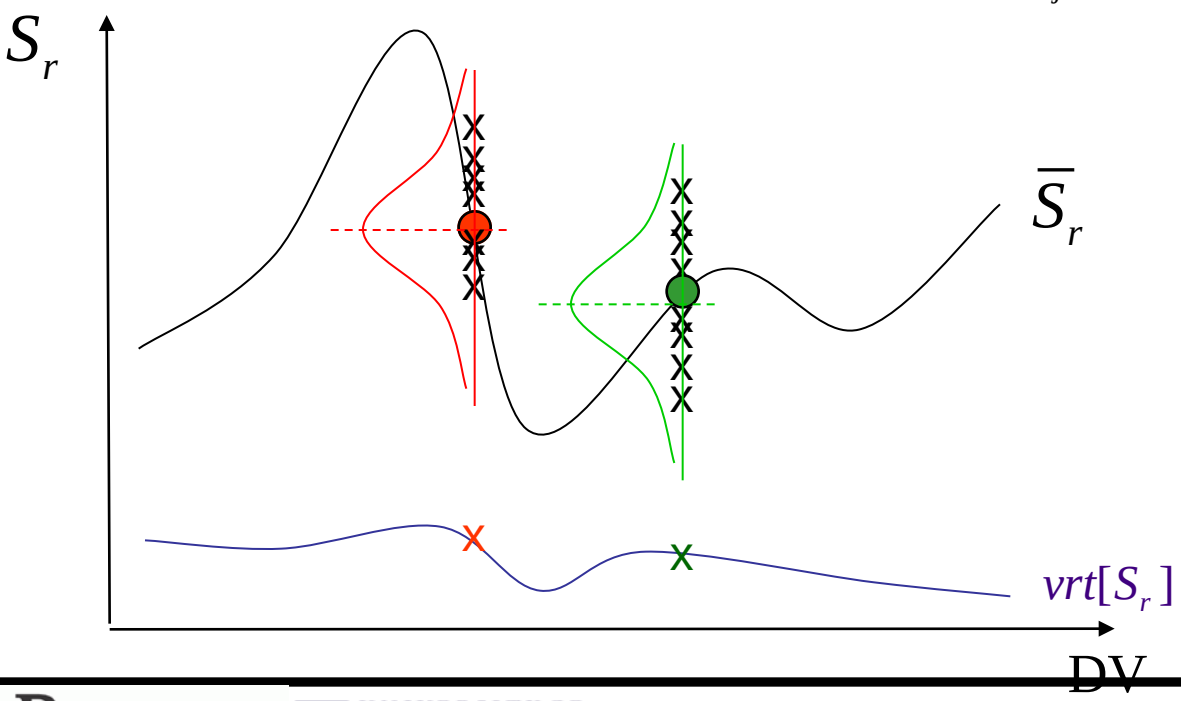

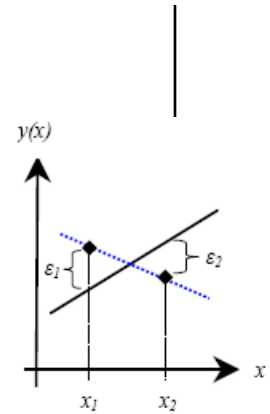

Figure 1. An illustration of the effect of random errors in producing an estimated linear model (dashed) that has a different slope than the true linear model (solid).

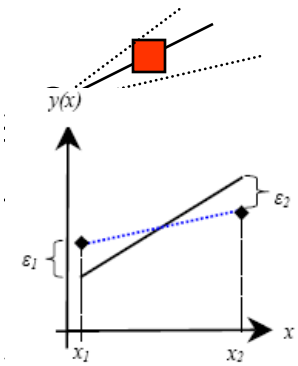

Figure 2. By moving the samples to the boundaries of the design space, the effect of the random error terms is reduced. Now, the estimated linear model (dashed) is a better approximation to the true linear model (solid).

Case 1. Results for α=1, with initial design x_o=[20, 10, 10, 4, 4, 5, 5], and strength value S_f=0.039321 *J*.

T=1500°C and α=1

Iteration	x_n	x_n^*	S_r	S_f
1	[20, 10, 10, 4, 4, 5, 5]	[16, 6, 8, 5, 5, 4, 4]	0.039628	0.039414
2	[16, 6, 8, 5, 5, 4, 4]	[12, 2, 7, 1, 5, 4, 3]	0.039552	0.039482
3	[12, 2, 7, 1, 5, 4, 3]	[10, 1, 1, 1, 4, 3, 2]	0.039540	0.039530
4	[10, 1, 1, 1, 4, 3, 2]	[10, 1, 1, 1, 5, 2, 4]	0.039535	0.039528
4	[10, 1, 1, 1, 4, 3, 2]	**(revaluate design and start using UQ in RSA)**		
5	[10, 1, 1, 1, 4, 3, 2]	[13, 1, 1, 1, 1, 5, 2]	0.039549	0.039497
6	[10, 1, 1, 1, 4, 3, 2]	**[10, 1, 1, 1, 4, 3, 2]**	0.039530	**0.039534**

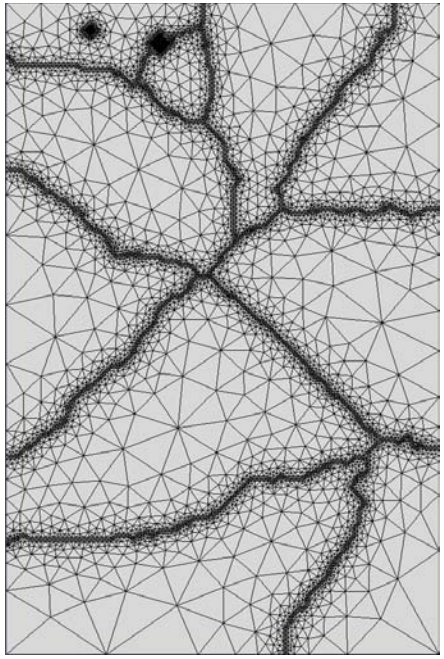

Iteration	ρ	ε_{f1}	ε_{f2}	ε_x	No. samples RSA (UQ Evaluations/sample)	No. samples Test TR (UQ Evaluations/sample)
1	0.30	2.06E-04	8.94E-05	0.181	66 (1)	1 (30)
2	0.49	6.78E-05	6.54E-05	0.186	49 (1)	1 (30)
3	0.83	9.59E-06	4.66E-05	0.167	49 (1)	1 (30)
4	-0.41	-	-	-	41 (1) 205	1 (30)
4	**(revaluate design and start using UQ in RSA)**					
5	-1.80	-	-	-	41 (30) 1230	1 (30)
6	25.09	**3.24E-06**	**3.38E-06**	**0.0**	65 (30) 1950	1 (30) 180

3565

Case 2. Results for α=0.5, with initial design x_o=[10, 1, 1, 1, 4, 3, 2], and strength value S_f = 0.0395237 *J*.

T=1500°C and α=0.5

Iteration	x_n	x_n*	S_r	S_f
5	[10, 1, 1, 1, 4, 3, 2]	[10, 1, 1, 3, 4, 3, 2]	0.0395253	0.0395239
6	[10, 1, 1, 3, 4, 3, 2]	**[10, 1, 1, 3, 4, 3, 2]**	0.0395251	**0.0395238**

Iteration	ρ	ε_{f1}	ε_{f2}	ε_x	No. samples RSA (UQ Evaluations/sample)	No. samples Test TR (UQ Evaluations/sample)
5	0.15	**1.35E-06**	**2.36E-07**	0.051	65 (30)	1 (30)
6	-0.13	**-**	**-**	**0.0**	62 (30)	1 (30)

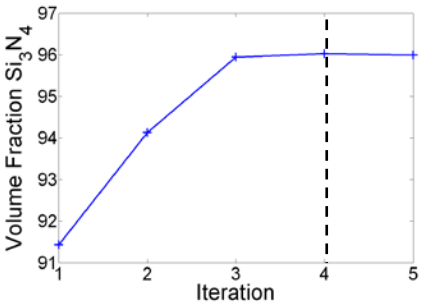

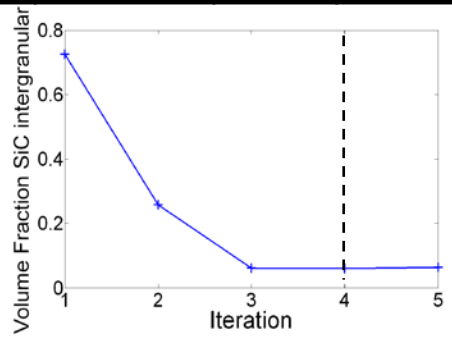

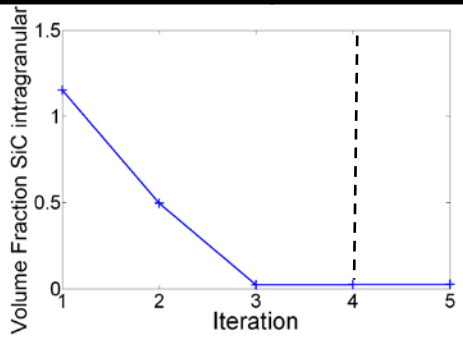

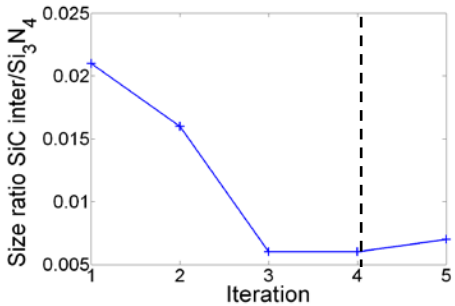

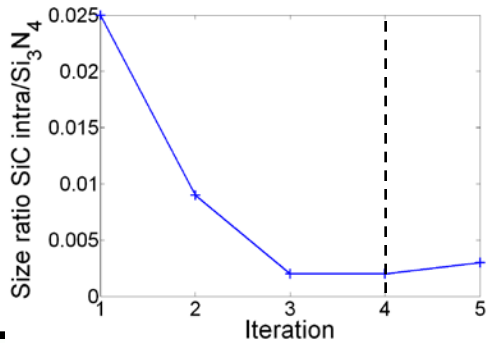

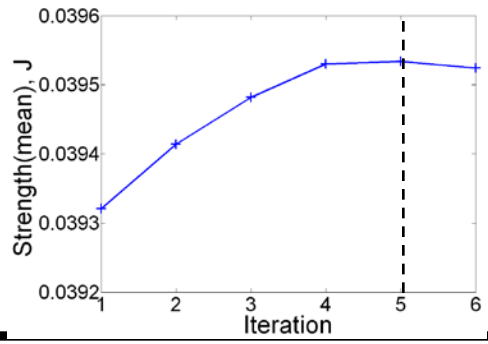

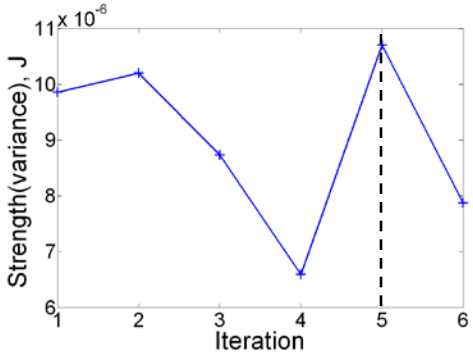

Case 3. Results for α=1, with initial design x_o=[25, 15, 15, 4, 4, 5, 5], and strength value S_f = 0.033152 *J*.

Iteration	x_n	x_n*	S_r	S_f
1	[25, 15, 15, 4, 4, 5, 5]	[21, 19, 21, 5, 5, 6, 6]	0.035251	0.033768
2	[21, 19, 21, 5, 5, 6, 6]	[23, 23, 23, 4, 6, 7, 7]	0.034218	0.034141
3	[23, 23, 23, 4, 6, 7, 7]	[32, 21, 28, 1, 7, 8, 8]	0.034765	0.034341
4	[32, 21, 28, 1, 7, 8, 8]	[40, 19, 35, 10, 10, 8, 8]	0.034661	0.034408
5	[40, 19, 35, 10, 10, 8, 8]	[40, 19, 35, 13, 10, 8, 8]	0.034639	0.034480
6	[40, 19, 35, 13, 10, 8, 8]	[40, 19, 35, 19, 10, 8, 8]	0.034663	0.034485
7	[40, 19, 35, 19, 10, 8, 8]	[40, 24, 35, 21, 10, 8, 8]	0.034706	0.034534
8	[40, 24, 35, 21, 10, 8, 8]	[40, 25, 36, 21, 9, 7, 7]	0.072728	0.034274
8	[40, 24, 35, 21, 10, 8, 8]	**(revaluate design and start using UQ in RSA)**		
9	[40, 24, 35, 21, 10, 8, 8]	[36, 23, 29, 21, 10, 8, 8]	0.034707	0.034502
10	[40, 24, 35, 21, 10, 8, 8]	**[40, 25, 36, 21, 10, 8, 8]**	0.034574	0.034569

T=1600ºC and α=1

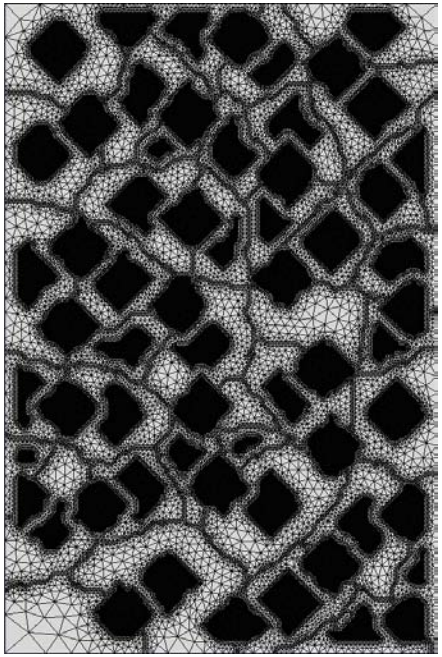

Iteration	ρ	ε_{f1}	ε_{f2}	ε_x	No. samples RSA (UQ Evaluations/sample)	No. samples Test TR (UQ Evaluations/sample)
1	0.29	1.43E-03	5.97E-04	0.18	66 (1)	1 (30)
2	0.83	7.45E-05	3.61E-04	0.19	33 (1)	1 (30)
3	0.32	4.10E-04	1.93E-04	0.33	25 (1)	1 (30)
4	0.21	2.45E-04	6.49E-05	0.33	49 (1)	1 (30)
5	0.31	1.54E-04	6.91E-05	0.08	65 (1)	1 (30)
6	0.03	1.72E-04	4.88E-06	0.15	50 (1)	1 (30)
7	0.22	1.65E-04	4.77E-05	0.21	49 (1)	1 (30)
8	-0.01	-	-	-	65 (1) 402	1 (30)
8	**(revaluate design and start using UQ in RSA)**					
9	-0.19	-	-	-	49 (30) 1470	1 (30)
10	0.88	**4.77E-06**	3.38E-05	**0.04**	61 (30) 1830	1 (30) 300 4002

Case 4. Results for α=0.5, with initial design x_o=[40, 25, 36, 21, 10, 8, 8], and strength value S_f=0.034563 *J*.

T=1600ºC and α=0.5

Iteration	x_n	x_n*	S_r	S_f
11	[40, 25, 36, 21, 10, 8, 8]	[36, 21, 29, 18, 9, 8, 8]	0.035187	0.034386
12	[40, 25, 36, 21, 10, 8, 8]	[40, 24, 36, 21, 9, 8, 8]	0.034566	0.034590
13	[40, 24, 36, 21, 9, 8, 8]	**[40, 24, 36, 21, 9, 8, 8]**	0.034595	0.034597

Iteration	ρ	ε_{f1}	ε_{f2}	ε_x	No. samples RSA (UQ Evaluations/sample)	No. samples Test TR (UQ Evaluations/sample)
11	-0.23	-	-	-	49 (30)	1 (30)
12	10.22	2.38E-05	2.63E-05	0.11	65 (30)	1 (30)
13	1.52	**2.31E-06**	**6.77E-06**	**0.0**	62 (30)	1 (30)

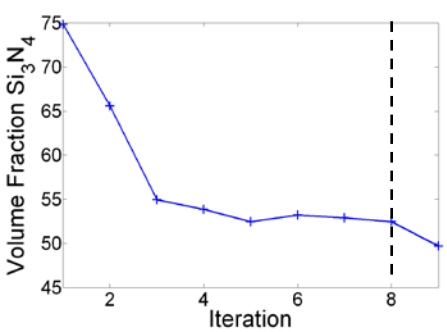

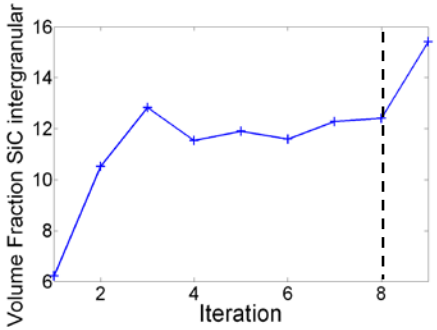

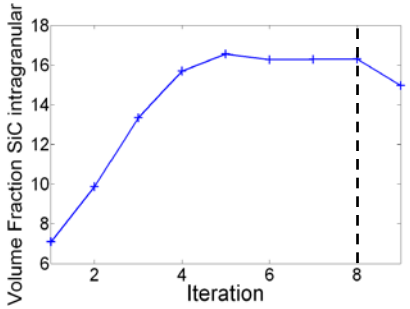

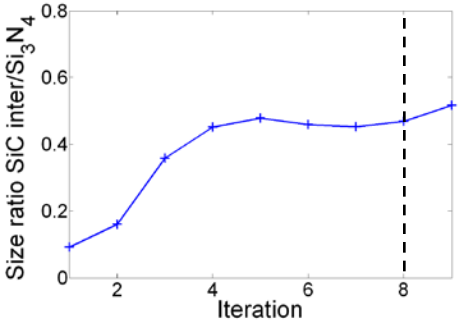

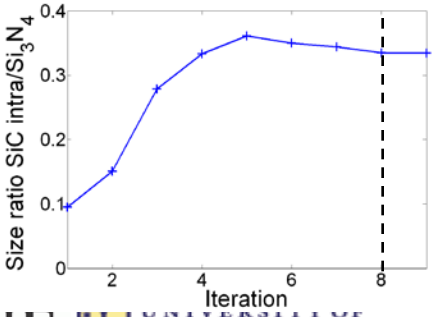

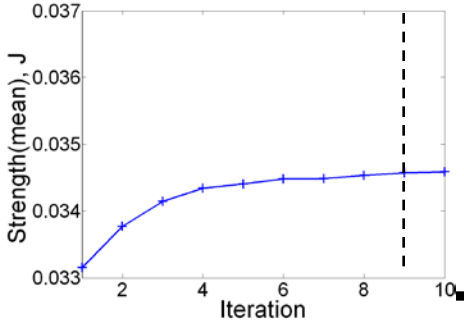

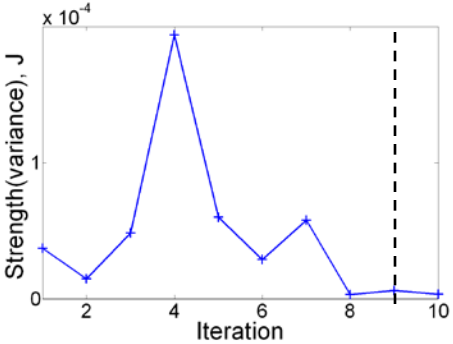

Case 5. Results for α=1, with initial design x_o=[20, 10, 15, 10, 5, 5, 5], and strength value S_{f_mo} = 0.427 *J*.

Iteration	x_n	x_n*	S_{r_mo}	S_{f_mo}
1	[25, 10, 15, 10, 5, 5, 5]	[25, 14, 15, 4, 4, 6, 6]	0.653	0.467
2	[25, 14, 15, 4, 4, 6, 6]	[25, 15, 16, 3, 5, 7, 7]	0.538	0.535
3	[25, 15, 16, 3, 5, 7, 7]	[23, 17, 19, 1, 5, 8, 8]	0.660	0.650
4	[23, 17, 19, 1, 5, 8, 8]	[19, 17, 19, 1, 5, 8, 8]	0.712	0.668
5	[19, 17, 19, 1, 5, 8, 8]	[15, 17, 15, 7, 4, 8, 8]	0.717	0.684
6	[15, 17, 15, 7, 4, 8, 8]	[11, 17, 11, 7, 4, 8, 8]	0.756	0.700
7	[11, 17, 11, 7, 4, 8, 8]	[10, 18, 10, 6, 4, 8, 8]	0.718	0.702
8	[10, 18, 10, 6, 4, 8, 8]	[10, 18, 10, 6, 4, 8, 7]	0.731	0.681
8	[10, 18, 10, 6, 4, 8, 8]	**(revaluate design and start using UQ in RSA)**		
9	[10, 18, 10, 6, 4, 8, 8]	**[10, 19, 10, 6, 4, 8, 8]**	0.740	0.703

Multiobjective, α=1
(w_1=0.5(1500°C)
(w_2=0.5(1600°C)

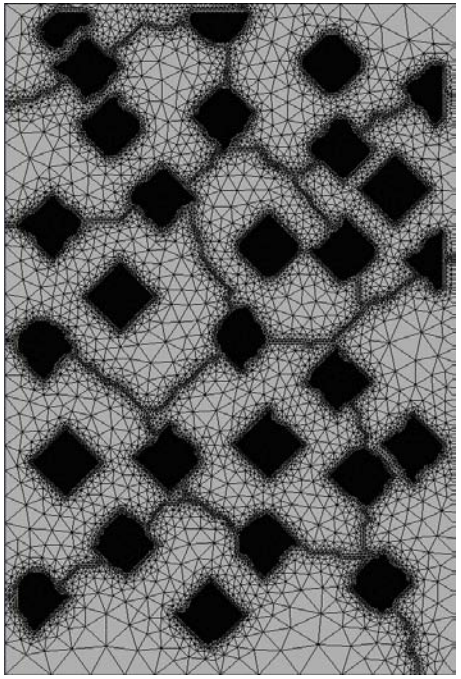

Iteration	ρ	ε_{f1}	ε_{f2}	ε_x	No. samples RSA (UQ Evaluations/sample)	No. samples Test TR (UQ Evaluations/sample)
1	0.18	1.27E-01	2.82E-02	0.22	66 (1)	1 (30)
2	0.96	2.02E-03	4.64E-02	0.18	65 (1)	1 (30)
3	0.92	6.21E-03	7.49E-02	0.18	65 (1)	1 (30)
4	0.28	2.67E-02	1.07E-02	0.13	49 (1)	1 (30)
5	0.33	1.96E-02	9.73E-03	0.15	33 (1)	1 (30)
6	0.23	3.28E-02	9.66E-03	0.13	25 (1)	1 (30)
7	0.11	9.12E-03	1.10E-03	0.04	48 (1)	1 (30)
8	-0.71	-	-	-	47 (1) 398	1 (30)
8	**(revaluate design and start using UQ in RSA)**					
9	0.03	2.18E-02	**6.17E-03**	**0.04**	49 (30) 1470	1 (30) 270 2138

Case 6. Results for α=0.5, with initial design x_o=[10, 18, 10, 6, 4, 8, 8], and strength value S_{f_mo} = 0.070199 *J*.

Iteration	x_n	x_n*	S_r	S_f
10	[10, 18, 10, 6, 4, 8, 8]	[10, 17, 9, 5, 4, 8, 8]	0.70307	0.70209
11	[10, 17, 9, 5, 4, 8, 8]	**[10, 17, 9, 5, 4, 8, 8]**	0.70210	0.70230

Multiobjective, α=0.5
(w_1=0.5(1500°C)
(w_2=0.5(1600°C)

Iteration	ρ	ε_{f1}	ε_{f2}	ε_x	No. samples RSA (UQ Evaluations/sample)	No. samples Test TR (UQ Evaluations/sample)
10	0.03	5.74E-04	1.76E-05	0.04	65 (30)	1 (30)
11	21	1.17E-04	1.23E-04	-	49 (30)	1 (30)

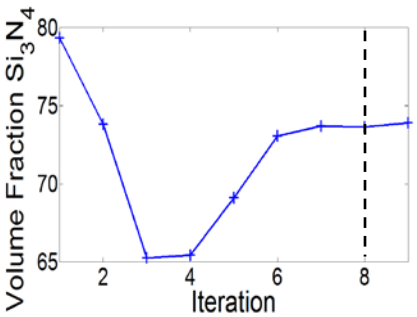

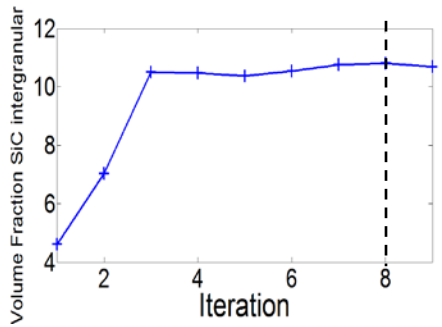

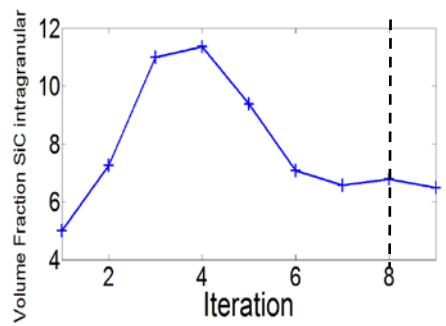

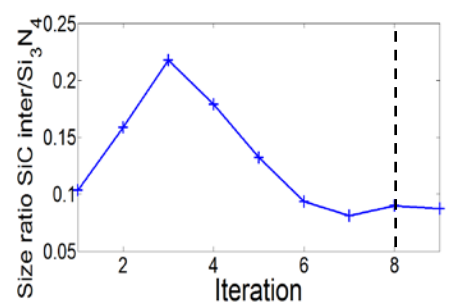

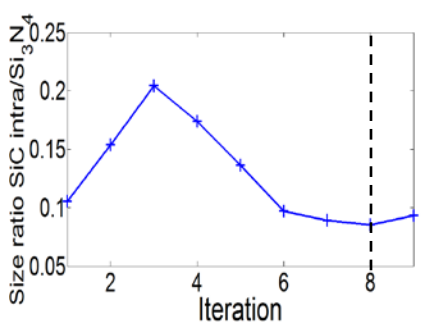

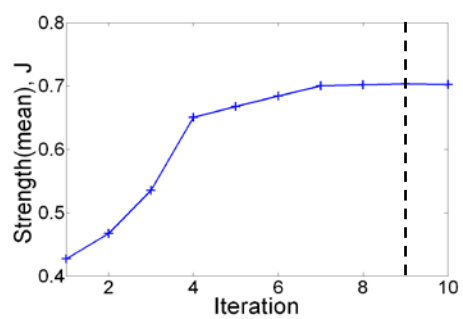

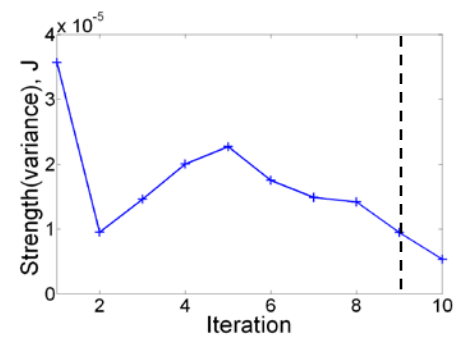

Summary

- Coal will become the energy and raw material resource of choice in the coming decades. The key is developing technologies for clean coal utilization. It is estimated that the use of bulk materials ($SiC-Si_3N_4$) with high temperature properties to operate at temperatures in excess of 1500 C in power plants can result in enhancements in the power generation efficiency by 10% to 15%.

- The Computer Aided Multiscale Design tool is expected to work efficiently on obtaining the most suitable sets of morphologies (design variables) to obtain a designated target set of properties by integrating multiscale simulations of the $SiC-Si_3N_4$ nanocomposite in a trust region variable fidelity framework.

- The tool is based on a sound combination of atomistic simulations, continuum simulations, and experiments in a design optimization framework

- The tool is efficient compared to existing approaches and has predicted many important insights about material behavior

Acknowledgements

- **We would like to once again thank DoE for the support.**

- **Refereed Archival Journal Publications**

1. Mejia-Rodriguez, G., Renaud, J.E., and Tomar V., 2010, Multiobjective composite material design using the variable fidelity model management optimization framework, in press in Engineering Optimization
2. Tomar, V., Gan, M., and Kim, H., 2010, Effect of temperature and morphology on mechanical strength of Si-C-O and Si-C-N nanocomposites, in press in the Journal of European Ceramic Society
3. Tomar, V., Samvedi, V., and Kim, H., 2010, Atomistic understanding of the particle clustering and particle size effect on the room temperature strength of SiC-Si3N4 nanocomposites to Appear in Int. J. Multiscale Comp. Engg. special issue on Advances In Computational Materials Science, volume 8 issue 4, 2010
4. Samvedi, V, and Tomar, V., 2008, Role of heat flow direction, monolayer film thickness, and periodicity in controlling thermal conductivity of a Si-Ge superlattice system, Journal of Applied Physics (featured in Virtual Journal of Nanoscale Science and Technology, volume 19, issue 4), vol 105, 013541
5. Tomar, V., and Samvedi, V, 2009, Atomistic simulations based understanding of the mechanism behind the role of second phase SiC particles in fracture resistance of SiC-Si3N4 nanocomposites, Vol 7, issue 4, 277-294 pages, International Journal of Multiscale Computational Engineering
6. Mejia-Rodriguez, G., Renaud, J.E., and Tomar V., 2008, A variable fidelity model management framework for designing multiphase materials, ASME J. Mech. Design, vol. 130, 091702-1
7. Tomar, V., 2008, Analyses of the role of the second phase SiC particles in microstructure dependent fracture resistance variation of SiC-Si_3N_4 nanocomposites, Modelling Simul. Mater. Sci. Eng. 16 (2008) 035001.
8. Tomar, V., 2007, Nanomechanical analyses of nanocrystalline Ni using accelerated molecular timesteps, Physica Status Solidi-a, vol. 204 (10), pp. 3340-3348.
9. Tomar, V., 2007, Accelerating the molecular timesteps for nanomechanical simulations: The hybrid Monte Carlo Method, Journal of Applied Physics, Vol. 101, pp 103512 (1-9)